

**L-Hydroxyproline and D-Proline Catabolism in *Sinorhizobium meliloti***

**By**

**SIYUN CHEN**

**July 18, 2014**

**A Thesis submitted to the School of Graduate Studies**

**for the Degree of Master of Science**

**McMaster University**

## **L-Hydroxyproline and D-Proline Catabolism in *Sinorhizobium meliloti***

MASTER OF SCIENCE (Chemical Biology 2014)

McMaster University

Hamilton, Ontario

TITLE: L-Hydroxyproline and D-Proline Catabolism in *Sinorhizobium meliloti*

AUTHOR: Siyun Chen, B.Sc (South China University of Technology)

SUPERVISOR: Dr. T. M. Finan

## ABSTRACT

Hydroxyproline as a modified amino acid can serve as a carbon and nitrogen source for certain microorganisms. Its primary isomer *trans*-4-hydroxy-L-proline is found in the root nodule of legume plants. Hydroxyproline (Hyp) catabolism has been characterized in bacteria and animal cells. In bacteria, *trans*-4-hydroxy-L-proline (*trans*-4-L-proline) is converted to the central metabolite  $\alpha$ -ketoglutarate ( $\alpha$ -KG) by four reactions. The Hyp catabolism pathway has been identified in the nitrogen-fixing legume endosymbiont *Sinorhizobium meliloti*. *hypS* is one of the transcripts in the 14 *hyp* gene cluster on the pSymB megaplasmid, and was annotated to encode a putative malate/L-lactate dehydrogenase. In this study, purified HypS was assayed on different substrates and the reaction products were characterized. It was demonstrated that HypS can oxidize L-proline and reduce  $\Delta^1$ -pyrroline-2-carboxylate, but not on L-malate. Noticeably unlike the wild type strain, a *hypS*<sup>-</sup> mutant strain failed to grow on D-proline. The ability of D-proline to support grow of an L-proline auxotroph, together with the substrate specificity of HypS, strongly suggests that *hypS* is involved in the metabolism of D-proline to L-proline in *S. meliloti*. The possible role of HypS in the catabolism of Hyp or related compounds remains to be determined.

## **ACKNOWLEDGEMENTS**

I would like to express my gratitude to Dr. Finan who provides me the opportunity to learn and work in his laboratory during the past two years and thank for his kind guidance and persistent help. I would also like to thank my committee members Dr. Britz-Mckibbin and Dr. Morton who provides suggestions and supports to my research. In addition, I would like to express my great appreciation to all my lab members to help and share their experiences to me, especially George diCenzo for sharing his strains and always giving me advices in the lab, and Ye Zhang for sharing his protein and advices on protein purification. I also thank ChemBio Admin, Tammy Feher, who helps me coordinate the administrative work in Department of Chemistry and Chemical Biology. I am also very grateful to my dear parents who support me to study in Canada and give me hope when I feel frustrations and encounter hard time.

## Contents

<b>ABSTRACT.....</b>	<b>I</b>
<b>ACKNOWLEDGEMENTS .....</b>	<b>II</b>
<b>LIST OF FIGURES.....</b>	<b>V</b>
<b>LIST OF TABLES .....</b>	<b>VI</b>
<b>INTRODUCTION .....</b>	<b>1</b>
<i>Sinorhizobium meliloti</i> .....	1
Hydroxyproline and proline .....	1
Metabolism of hydroxyproline.....	5
HypS: a putative malate/L-lactate dehydrogenase .....	10
This Work .....	11
<b>MATERIAL AND METHODS .....</b>	<b>13</b>
Bacterial strains, media and growth condition .....	13
Transduction .....	14
Conjugation.....	14
Transformation .....	15
Construction of the $\Delta araE$ , $\Delta hypH$ double mutant.....	15
Reintroducing <i>hypS</i> <sup>+</sup> into the $\Delta hypS$ mutant strain .....	15
Proline auxotroph .....	16
<i>hyp</i> gene expression.....	16
Growth in liquid media.....	17
Synthesis of $\Delta^1$ -pyrroline-2-carboxylate.....	17
Sample preparation and direct infusion in Mass Spectrometer .....	18
Synthesis of $\Delta^1$ -pyrroline-4-hydroxy-2-carboxylate .....	19
HypS Enzymatic assay .....	19
Amino acids alignment and phylogenetic analysis .....	20
Determine the concentration of $\alpha$ -KGSA stock solution.....	20
12% SDS Polyacrylamide Gel Electrophoresis .....	21

BL21/DE3 pLysS competent cell .....	21
Purification of HypD .....	22
<b>RESULTS.....</b>	<b>24</b>
Enzymatic synthesis of $\Delta^1$ -pyrroline-2-carboxylate.....	24
$\Delta^1$ -pyrroline-2-carboxylate reduction by purified HypS.....	25
Products formed from the HypS and NADPH-dependent reduction of $\Delta^1$ -pyrroline-2-carboxylate .....	26
Substrate of HypS (Oxidation).....	27
Cofactor .....	28
Kinetics Analysis of HypS .....	29
pH effect.....	31
<i>hypS</i> is involved in D-proline metabolism.....	32
Growth of $\Delta hypS$ mutant on D-proline .....	32
Growth of $\Delta hypS$ mutant in liquid media. ....	34
<i>hyp</i> genes expression .....	35
<i>putA</i> <sup>-</sup> mutant .....	36
How is D-proline transported into the cells .....	37
Are other <i>hyp</i> genes involved in D-proline catabolism .....	38
HypS can also reduce $\Delta^1$ -Piperidine-2-carboxylate.....	39
<i>S.meliloti</i> was tested on different carbon sources .....	40
Amino acid alignment and phylogenetic analysis .....	41
Growth of $\Delta hypO, D, H, S$ mutant .....	45
HypH: KGSA dehydrogenase	
Growth of $\Delta araE \Delta hypH$ double mutant in liquid media .....	45
Enzymatic characterization of HypH .....	46
Purification of recombinant protein HypD .....	49
HypD enzymatic assay : Couple assay with HypH .....	51
HypO couple assay with HypS on <i>cis</i> -4-D-Hyp .....	53
<b>CONCLUSION AND DISCUSSION.....</b>	<b>55</b>
<b>APPENDIX.....</b>	<b>59</b>
<b>REFERENCE .....</b>	<b>65</b>

## List of Figures

<b>Figure 1.</b> 4-Hydroxyproline isomers .....	<b>2</b>
<b>Figure 2.</b> The catabolic pathway of hydroxyproline in bacteria .....	<b>7</b>
<b>Figure 3.</b> Schematic of the <i>hyp</i> gene cluster found on pSymB of <i>S.meliloti</i> .....	<b>7</b>
<b>Figure 4.</b> Identification of the product of D-proline by DAAO.....	<b>25</b>
<b>Figure 5.</b> Relationship between absorbance and time .....	<b>26</b>
<b>Figure 6.</b> Identification of the product of pyrroline-2-carboxylate by HypS .....	<b>27</b>
<b>Figure 7.</b> HypS enzyme kinetics .....	<b>30</b>
<b>Figure 8.</b> pH effect on the activity of HypS.....	<b>31</b>
<b>Figure 9.</b> Schematic of <i>hypS</i> gene reintroducing into <i>hypS</i> <sup>-</sup> mutant strain .....	<b>32</b>
<b>Figure 10.</b> Growth of $\Delta hypS$ mutant in M9 minimum media with various carbon source ...	<b>35</b>
<b>Figure 11.</b> Grow curve of a <i>putA</i> <sup>-</sup> mutant with different carbon sources .....	<b>37</b>
<b>Figure 12.</b> Grow curve of <i>hypMNPQ</i> mutant with various carbon sources .....	<b>38</b>
<b>Figure 13.</b> Grow curve of other <i>hyp</i> mutant with various carbon sources .....	<b>39</b>
<b>Figure 14.</b> Relationship between absorbance and time .....	<b>40</b>
<b>Figure 15.</b> Unrooted neighbour joining tree of Ldh_2 family .....	<b>42</b>
<b>Figure 16.</b> Multiple sequence alignment of DpkA clade .....	<b>43</b>
<b>Figure 17.</b> Grow curve in M9 minimum media supplemented with various carbon source .	<b>46</b>
<b>Figure 18.</b> Relationship between absorbance and time .....	<b>47</b>
<b>Figure 19.</b> HypH enzyme kinetics .....	<b>48</b>
<b>Figure 20.</b> SDS-PAGE gel analysis of the HypD over-expression in whole cell extracts .....	<b>49</b>
<b>Figure 21.</b> SDS-PAGE gel analysis of the HypD purification .....	<b>50</b>
<b>Figure 22.</b> SDS-PAGE gel analysis of the HypD purification .....	<b>51</b>
<b>Figure 23.</b> Relationship between absorbance and time .....	<b>52</b>
<b>Figure 24.</b> Relationship between absorbance and time with HypO, HypD, HypH on <i>cis</i> -4-D-Hyp.....	<b>53</b>
<b>Figure 25.</b> Relationship between absorbance and time on HPC catalyzed by HypS.....	<b>54</b>
<b>Figure 26.</b> Schematic diagram showing the reaction between L-proline and Pyr2C .....	<b>55</b>
<b>Figure 27.</b> Schematic of gene clusters related to 4-hydroxyproline catabolism of bacteria ..	<b>58</b>
<b>Figure 28.</b> Growth of <i>hypS</i> mutant, L-proline auxotroph, and its derivative on minimum agar	

plate .....	61
<b>Figure 29.</b> Protein Standard curve (BSA) by using Bio-Rad protein assay .....	<b>62</b>
<b>Figure 30.</b> Schematic of FPLC system connection.....	<b>63</b>
<b>Figure 31.</b> Chromatogram of fraction 2&3.....	<b>63</b>
<b>Figure 32.</b> Schematic of gene fusions .....	<b>64</b>

## List of Tables

<b>Table 1.</b> New family of NAD(P)H-dependent oxidoreductases .....	<b>11</b>
<b>Table 2.</b> Substrate specificity .....	<b>28</b>
<b>Table 3.</b> Cofactor .....	<b>28</b>
<b>Table 4.</b> Kinetic parameters of HypS .....	<b>31</b>
<b>Table 5.</b> Growth of <i>S.meliloti</i> on M9 plate with various carbon and nitrogen .....	<b>33</b>
<b>Table 6</b> <i>hyp</i> genes expression .....	<b>35</b>
<b>Table 7.</b> Growth of wild type <i>S.meliloti</i> on different carbon sources .....	<b>40</b>
<b>Table 8.</b> Percent Identity Matrix.....	<b>44</b>
<b>Table 9.</b> Growth of $\Delta hypRE, O, D, H, S$ mutant with <i>trans</i> -4-L-Hyp .....	<b>45</b>
<b>Table 10.</b> The kinetic parameters of HypH .....	<b>49</b>
<b>Table 11.</b> Protein concentration of each step .....	<b>51</b>
<b>Table 12.</b> Strains and plasmids used in this study .....	<b>59</b>
<b>Table 13.</b> Protein concentration of each eluted fractions .....	<b>62</b>

# INTRODUCTION

## *Sinorhizobium meliloti*

Rhizobia are nitrogen-fixing bacteria that participate in a symbiotic relationship with host plants in the legume family. Flavonoids released from the roots of host plant induce transcription of the structural *nod* genes in rhizobia and the nod proteins synthesize the lipochito-oligosaccharide Nod factor. (Cooper, 2007; Geurts and Bisseling, 2002). The Nod factors in return induce the curling of root hair cells and formation of root nodules (Geurts et al., 2005).

*Sinorhizobium meliloti* is gram-negative alpha-proteobacterium, with a genome that consists of a 3.7kb chromosome, the 1.4 kb pSymA megaplasmid and the 1.7 kb pSymB megaplasmid. The host plant benefits from the nitrogen fixation by the bacteroid within nodules. The plant offers carbon and nitrogen sources for the bacteria to grow within the nodules (Long, 2001). Hydroxyproline is one of the carbon and nitrogen sources that can be catabolized by *S. meliloti* (Maclean et al., 2009a).

## Hydroxyproline and proline

Hydroxyproline (Hyp) is a modified amino acid which has three kinds of stable isomers, 4-hydroxyproline, 3-hydroxyproline and 3,4-dihydroxyproline (Adams and Frank, 1980). Here, we focus on 4-hydroxyproline. As 4-hydroxyproline has two chiral carbon, there are four kinds of isomers of 4-hydroxyproline dependent on the two different chiral carbons. They are *trans*-4-L-Hyp, *cis*-4-D-Hyp, *trans*-4-D-Hyp and *cis*-4-L-Hyp (Figure.1). (2S,4R)-4-hydroxyproline, which is also called *trans*-4-hydroxy-L-proline (*trans*-4-L-Hyp), is

abundant in collagen in animal protein. About 4% of the total amino acids in animal acids is *trans*-4-L-Hyp (Gorres and Raines, 2010). *Trans*-4-L-Hyp is formed by the post-translational hydroxylation of L-proline by procollagen-proline dioxygenase (prolyl hydroxylase) (EC 1.14.11.2). However, in microbial systems, free *trans*-4-L-Hyp is hydroxylated from free L-proline by proline 4-hydroxylase (Shibasaki et al., 1999).

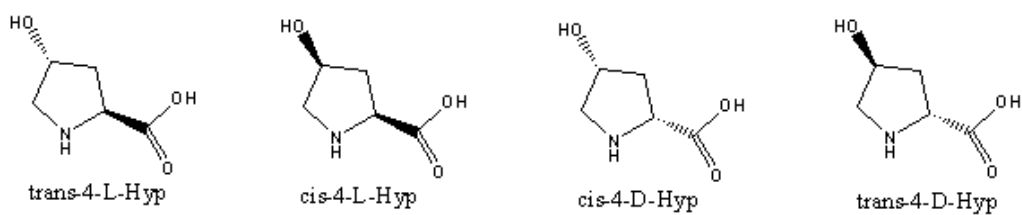


**Figure 1. 4-Hydroxyproline isomers**

In addition to collagen, it is also found in other proteins, such as elastin, conotoxins, and argonaute which have a collagen-like domains (Gorres and Raines, 2010). In plants, hydroxyproline is the major component in hydroxyproline-rich glycoproteins (HRGP) in plant cell wall. HRGP are not only essential to the interactions between cells in recognition processes, but also play a critical role in many functional activities. At least three kinds of hydroxyproline-rich glycoproteins (HRGP) were known. These are lectin-like proteins, arabinogalactan proteins and extensins (Khashimova, 2003). Roots of legume plants are rich in hydroxyproline which is found in extensin proteins (Frueauf et al., 2000). As a class of plant glycoprotein, root nodule extensin in pea nodule is localized to the infection thread lumen (Rathbun et al., 2002). Hydroxyproline is abundant in pea mucilage which secreted from the plant roots provides a potential source of carbon to the microbes around the

rhizosphere, such as *Rhizobium leguminosarum*, *Burkholderia cepacia*, and *Pseudomonas fluorescens* (Knee et al., 2001).

The hydroxyproline isomer *cis*-4-L-Hyp has been reported to be synthesized from free L-proline by microbial L-proline *cis*-4-hydroxylase (EC 1.14.11). Proteins from *Mesorhizobium loti* and *S. meliloti* have been detected to have this enzymatic function. The gene in *S. meliloti* is designated as *Smc03253* (Hara and Kino, 2009) and the transcription of this gene is induced in the nodule and its expression is regulated by FixJ (Ferrieres et al., 2004).

In addition, *trans*-3-L-hydroxyproline noticeably exists in collagen IV, which is an essential structural component of basement membrane. It has been reported that the C14orf149 from human is a *trans*-3-L-Hyp dehydratase (EC 4.2.1.77) that catalyzes the dehydration of *trans*-3-L-Hyp to  $\Delta^1$ -pyrroline-2-carboxylate (Pyr2C), which is subsequently metabolized to L-proline. *Trans*-3-L-Hyp dehydratase has been reported to be present in fungi and animals (Visser et al., 2012a) and recently found in *Azospirillum brasilense* (Watanabe et al., 2014).

It was recently reported that the hydroxyproline derivative *trans*-4-hydroxy-L-proline-betaine (tHyp-B) and *cis*-4-hydroxy-D-proline betaine (cHyp-B) are catabolized via a pathway that includes the steps through which Hyp is converted to  $\alpha$ -ketoglutarate. Betaines are quaternary amino derivatives of amino acids, which are accumulated when cells encounter unfavourable environments. It is predicted that a hydroxyproline-betaine 2-epimerase converts tHyp-B to cHyp-B which is subsequently demethylated to N-methyl cHyp. A flavin-dependent enzyme converts N-methyl cHyp to cHyp. Finally cHyp goes into the identified hydroxyproline catabolic pathway to make

$\alpha$ -ketoglutarate (Zhao et al., 2013). In addition, proline betaine (Pro-B) also accumulate at high stress in plants and marine algae. The Pro-B degradation pathway was also recently described and it shares several of key enzymes of hydroxyproline betaine catabolic pathway. The hydroxyproline-betaine 2-epimerase is also active on the racemization of the L-Pro-B to D-Pro-B (Kumar et al., 2014).

Besides hydroxyproline, L-proline is clearly essential for protein synthesis, structure, metabolism and nutrition (Wu et al., 2011). L-proline is synthesized from glutamate via  $\Delta^1$ -pyrroline-5-carboxylate (Adams and Frank, 1980). The L-amino acid enantiomer predominates in living cells and is used in the ribosomal synthesis of proteins and plays a critical role in metabolism in cells. D-amino acids are found in bacteria and have become increasingly interesting in bacterial physiology, even though not much is known about their synthesis and metabolism (Radkov and Moe, 2013). *Vibrio cholerae* produces D-Met and D-Leu and *Bacillus subtilis* produces D-Tyr and D-Phe. These D-amino acids are important for the synthesis of peptidoglycan, including its composition, amount and strength. D-amino acids may coordinate the metabolic slowing in cell wall and cytoplasmic compartments when it is in scarce resource situations. This helps bacteria to adapt to a changing environment (Lam et al., 2009). In *Salmonella typhimurium*, D-histidine in peptides prolongs the life of peptides which enhances the antimicrobial activity (Nishikawa and Ogawa, 2004). D-amino acid oxidase (DAAO, EC 1.4.3.3) which is a flavin enzyme, is able to oxidize D-amino acids to yield  $\alpha$ -imino acids, that are subsequently hydrolyzed to  $\alpha$ -keto acids. The electron acceptor is dioxygen (Pollegioni et al., 1997).

## Metabolism of Hydroxyproline

In mammals, four mitochondrial enzymes are involved in 4-hydroxyproline metabolism. *trans*-4-L-Hyp is oxidized to  $\Delta^1$ -pyrroline-3-hydroxy-5-carboxylate (Pyr3H5C) by hydroxyproline oxidase (HPOX). Subsequently Pyr3H5C is converted to 4-hydroxyglutamate by  $\Delta^1$ -pyrroline-5-carboxylate dehydrogenase (1P5CDH). Furthermore, 4-hydroxyglutamate is oxidized to 4-hydroxy-2-oxoglutarate (HOG) by aspartate aminotransferase (AspAT). The final product of the L-hydroxyproline degradation is pyruvate and glyoxylate, which are produced from HOG by 4-hydroxy-2-oxoglutarate aldolase (HOGA, EC 4.1.3.16) (Riedel et al., 2011). The hydroxyproline pathway in mammals is linked to the general L-proline pathway, as some intermediates are the same. L-proline is converted to  $\Delta^1$ -pyrroline-5-carboxylate (Pyr5C) by L-proline dehydrogenase (L-PDH; EC 1.5.99.8), which is a flavin adenine dinucleotide (FAD)-dependent oxidation. Pyr5C is spontaneously hydrolyzed to glutamate  $\gamma$ -semialdehyde and is subsequently oxidized to L-glutamate by Pyr5C dehydrogenase (Menzel and Roth, 1981).

In bacteria, the hydroxyproline pathway was investigated through studies of *Pseudomonas* strains isolated from soil that grew on *trans*-4-hydroxy-L-proline as a carbon source (Adams and Frank, 1980). The bacterial catabolic pathway is different from the pathway in mammals. In bacteria, there are four enzymes and four enzymatic reactions involved in the degradation of L-hydroxyproline to  $\alpha$ -ketoglutaric acid ( $\alpha$ -KG), which is an intermediate in tricarboxylic acid (TCA) cycle. The isomerization of *trans*-4-L-Hyp to *cis*-4-D-Hyp is catalyzed by hydroxyproline-2-epimerase (EC 5.1.1.8). Afterwards, *cis*-4-D-Hyp is oxidized to  $\Delta^1$ -pyrroline-4-hydroxy-2-carboxylate (HPC) by a hydroxyproline specific

D-amino acid oxidase (EC 1.4.3.3). HPC is converted to  $\alpha$ -ketoglutarate semialdehyde ( $\alpha$ -KGSA) by  $\Delta^1$ -pyrroline-4-hydroxy-2-carboxylate deaminase (EC 3.5.4.22). The final product is  $\alpha$ -ketoglutaric acid ( $\alpha$ -KG) produced from  $\alpha$ -KGSA by  $\alpha$ -KGSA dehydrogenase (KGSADH, EC 1.2.1.26) (Adams and Frank, 1980; Singh and Adams, 1964; Yoneya and Adams, 1961). Among all five compounds,  $\Delta^1$ -pyrroline-4-hydroxy-2-carboxylate (HPC) will hypothetically open its ring to become a chain compound 2-oxo-4-hydroxy-5-aminovalerate (Singh and Adams, 1965).

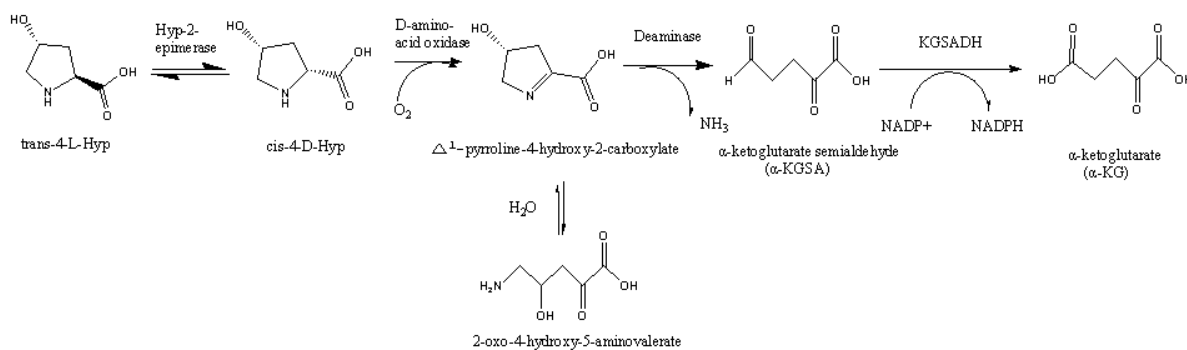


**Figure 2.** The catabolic pathway of hydroxyproline in bacteria, which involves four reactions of the conversion from *trans*-4-L-Hyp to  $\alpha$ -ketoglutaric acid (Singh and Adams, 1965).

A cluster of 14 *hyp* genes that constitute hydroxyproline catabolism locus on the pSymB megaplasmid of *S. meliloti* has been identified recently. There are five transcripts in the cluster, three with a single gene, one with two genes and one containing nine genes. This cluster includes an ABC-transport system encoded by the gene *hypMNPQ*, a negative regulator encoded by *hypR*, as well as six genes with putative functions and three ORFs (*hypT*, *hypX*, *hypZ*) without predicted function.

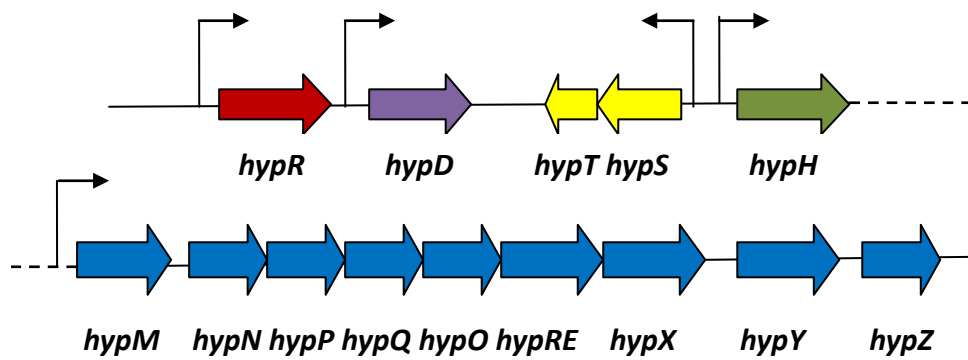


**Figure 3.** Schematic of the *hyp* gene cluster from the pSymB megaplasmid of *S. meliloti* (White et al., 2012a)

Four of the predicted enzymes, *trans*-4-hydroxy-L-proline epimerase encoded by *hypRE*, D-amino acid oxidase encoded by *hypO*, deaminase encoded by *hypD* and  $\alpha$ -ketoglutaric semialdehyde dehydrogenase encoded by *hypH*, comprise the reactions in the predicted pathway. HypRE (hydroxyproline-epimerase) enzyme is a racemase containing two conserved cysteine residues in the active site. It catalyzes the isomerization of *trans*-4-L-proline to *cis*-4-D-proline (White et al., 2012a). HypO (D-amino acid oxidase) enzyme is also called allohydroxy-D-proline oxidase in studies with *P. striata* (Yoneya and Adams, 1961), and called allohydroxy-D-proline dehydrogenase in studies with *P. aeruginosa* (Bater et al., 1977). In particular, it is a cytochrome-linked oxidase involving oxygen, as the hydroxyproline-reduced cytochromes are reoxidisable by oxygen through cytochromes oxidase. Furthermore, it is highly substrate specific, which is quite different from other D-amino acid oxidases (Bater et al., 1977; Yoneya and Adams, 1961). HypO catalyzes the reaction from *cis*-D-hydroxyproline, which is rare in nature, to  $\Delta^1$ -pyrroline-4-hydroxy-2-carboxylate (HPC). Despite its hypothetical open chain, HPC is

stable in high alkaline conditions (pH 11)(Singh and Adams, 1965). Nonetheless it will spontaneously degrade to pyrrole-2-carboxylic acid (PYC) in acidic conditions. HPC is not commercially available. Singh and Adams synthesized HPC from *cis*-4-D-Hyp (Singh and Adams, 1965). Yoneya and Adams suggested that hydrogen peroxide is not produced and that the oxidation reaction is linked to cytochrome reduction. Interestingly, phenazine methosulfate (PMS) is used to produce HPC. However, the role of PMS remains unclear whether it is an electron donor to reduce oxygen directly or an electron carrier (Yoneya and Adams, 1961). HypD (deaminase) which belongs to the dihydrodipicolinate synthase/N-acetylneuraminase lyase family, catalyzes the deamination of the pyrroline ring to a carbon chain  $\alpha$ -ketoglutarate semialdehyde (Watanabe et al., 2012; White et al., 2012a). HypH (ketoglutarate semialdehyde dehydrogenase) is involved in the last step to catalyze the conversion from  $\alpha$ -KGSa to  $\alpha$ -KG.  $\alpha$ -KGSADH belongs to aldehyde dehydrogenase (ALDH) superfamily. There are three different kinds of  $\alpha$ -KGSADH were characterized in *Azospirillum brasilense*, including L-arabinose-related enzyme KGSADH-I, D-glucarate/D-galactarate-inducible NAD<sup>+</sup>-dependent KGSADH-II and hydroxy-L-proline-inducible NADP<sup>+</sup>-KGSADH-III. *A. brasilense* KGSADH-I belongs to type I KGSADH. Both *A. brasilense* KGSADH-II and KGSADH-III belong to type II KGSADH. In addition, ycbD KGSADH protein from *B. subtilis* belong to type III. It showed a distant phylogenetic relationship to type I, II and III (Watanabe et al., 2007).

*S. meliloti* is capable of utilizing hydroxyproline as carbon and nitrogen source (White et al., 2012a). Previous data showed that *hypMNPQ* encoded an ABC-transport system for the high affinity uptake of *trans*-4-L-Hyp. It is induced by both *trans*-4-L-Hyp and *cis*-4-D-Hyp.

*Cis*-4-D-Hyp less effectively inhibited the uptake of *trans*-4-L-Hyp than either *trans*-4-L-Hyp itself or L-proline. The finding also suggested that the L-proline ABC transport system can also transport hydroxyproline (Maclean et al., 2009a). In *P. putida*, the transport system will also preferentially take up *trans*-4-L-Hyp over *cis*-4-D-Hyp (Gryder and Adams, 1970). However, in *P. aeruginosa* PAO, it failed to uptake *cis*-4-D-Hyp due to the permeability barrier unless it was treated by EDTA (Manoharan, 1980).

Transcript start sites were identified upstream of *hypR*, *hypD*, *hypS*, *hypH*, *hypM* by using primer extension analysis. These sites are 16 nucleotides, 69 nucleotides, 51 nucleotides, 166 nucleotides and 38 nucleotides upstream of each predicted start codon (White et al., 2012a). The transcripts all negatively regulated by *hypR*, which is a member of the helix–turn–helix GntR (FadR) family of transcription regulators. FadR consists of all-helical C-terminal domains with seven  $\alpha$ -helices (Rigali et al., 2002). Each promoter is repressed by HypR in the absence of hydroxyproline. However, the repression is relieved at the presence of either *trans*-4-L-Hyp or *cis*-4-D-Hyp (White et al., 2012a).

### **HypS: a putative malate/L-lactate dehydrogenase**

The NAD(P)-dependent malate (L-MalDH) and NAD-dependent lactate (L-LDH) dehydrogenase family comprise a large super-family whose members have been characterized from Archae, Bacteria and Eukaryotes. The phylogenetic trees of the whole super-family showed three different groups, L-LDH, [LDH-like] L-MalDH, and dimeric L-MalDH (Madern, 2002). Malate dehydrogenase catalyzes the interconversion between malate and oxaloacetate, while L-lactate dehydrogenase catalyzes interconversion between

L-lactate and pyruvate. However, a new class of malate/L-lactate dehydrogenase was found to show strikingly lower sequence similarity to other known MDH and LDH of eubacteria and eukaryotes. The L-Malate dehydrogenase from the extremely thermophilic methanogen *Methanothermobacter feravidus*, possesses low specificity for NAD<sup>+</sup> or NADP<sup>+</sup> and catalyzes preferentially the reduction of oxaloacetate. Meanwhile, another L-lactate dehydrogenase in *Alcaligenes eutrophus* showed 29% identity to MDH in *Methanothermobacter feravidus* (Honka et al., 1990; Jendrossek et al., 1993). This new kind of MDH and LDH are distinctive from the traditional proteins, as they showed different substrate specificity to other than MDH or LDH. Therefore, this kind of protein is annotated as a type-2 malate/L-lactate dehydrogenase. The new protein family has no GXGXX(G/A) sequence motif characteristic of the Rossmann fold. Previously, it has been grouped into eight clades, including various enzymes with unique catalytic activities other than MDH or LDH activity (Muramatsu et al., 2005a).

**Table 1. New family of NAD(P)H-dependent oxidoreductases (Muramatsu et al., 2005a)**

Clade	Organism	Protein function
ComC	<i>Methanothermobacter feravidus</i>	L-sulfolactate dehydrogenase
	<i>Methanobacterium thermoautotrophicum</i>	
	<i>Methanocaldococcus jannaschii</i>	
	<i>Methanocaldococcus jannaschii</i>	
AlID	<i>Escherichia coli</i>	ureidoglycolate dehydrogenase
	<i>Bacillus subtilis</i>	
	<i>Salmonella typhimurium</i>	
YiaK	<i>Escherichia coli</i>	2,3-diketo-L-gulonate reductase
	<i>Pasteurella multocida</i>	
	<i>Haemophilus influenza</i>	
DpKA	<i>Pseudomonas putida</i>	Pip2C/Pyr2C reductase
	<i>Pseudomonas syringae</i>	
	<i>Pseudomonas aeruginosa</i>	
LDH	<i>Alcaligenes eutrophus</i>	L-lactate dehydrogenase
	<i>Escherichia coli</i> O6	

Thermophilic archaeal	<i>Pyrococcus horikoshii</i> <i>Pyrococcus abyssi</i>	Uncharacterized proteins
YbiC	<i>Escherichia coli</i> <i>Bradyrhizobium japonicum</i>	Uncharacterized proteins
YlbC	<i>Drosophila melanogaster</i> <i>Caenorhabditis elegans</i>	Uncharacterized proteins

Among the 14 *hyp* genes of *S. meliloti*, *hypS* (*smb20261*) is located from 265534 to 266571 on pSymB megaplasmid, and encodes a 345 amino acid putative protein. This is annotated as a malate/L-lactate dehydrogenase in various proteins data bases. Both the *hypS* and *hypH* transcripts share an overlapping HypR binding site, which is upstream of the 10 region of the *hypS* and *hypH* promoters. *hypS* is induced in the presence of either *trans*-4-L-Hyp or *cis*-4-D-Hyp, but is not induced by other carbon sources, such as glucose, glycerol, succinate or L-proline (White et al., 2012a). In unpublished experiments in Dr. Finan's laboratory, Ye Zhang overproduced and purified a His-tagged HypS protein to homogeneity.

### **This Work:**

The goal of this study was to investigate the biological function of HypS, HypD and HypH in *S. meliloti*. We also examined the phenotype of *hypO* mutants and investigate the role of HypS in the synthesis of L-proline from D-proline but not *trans*-4-L-Hyp or *cis*-4-D-Hyp *in vivo* in free-living cells.

To test the substrate specificity and enzyme activity of HypS, a variety of amino acids were used for the enzyme assays. The enzyme showed activity on the oxidation of L-proline and the reduction of  $\Delta^1$ -pyrroline-2-carboxylate (Pyr2C), but no L-malate dehydrogenase

activity. HypS is a NADP(H)-dependent enzyme, and preferentially converts from Pyr2C to L-proline. Interestingly, a *hypS*<sup>-</sup> mutant was unable to grow with D-proline as a carbon and nitrogen source. In contrast, *hypS*<sup>-</sup> mutant was able to grow on hydroxyproline as a carbon and nitrogen source. It is interesting to know that in *Pseudomonas putida*, a gene *dpkA* annotated as  $\Delta^1$ -piperideine-2-carboxylate/ $\Delta^1$ -pyrroline-2-carboxylate reductase has been characterized and grouped as a member of a novel subclass in a large protein family of NAD(P)-dependent oxidoreductases (Muramatsu et al., 2005b). HypS showed 40% identity with DpkA by amino acid sequence alignment.

## MATERIAL AND METHODS

### Bacterial strains, media and growth condition

The *S. meliloti* and *E. coli* strains used in this study were summarized and listed in Table 12. *S. meliloti* strains were grown in Luria-Bertani (LB) broth supplemented with 2.5 mM CaCl<sub>2</sub> and 2.5 mM MgSO<sub>4</sub> (LBmc) or on LB agar plates incubated at 30°C. *E. coli* was grown in LB broth or LB agar plate incubated at 37°C. The concentration of antibiotics for *S. meliloti* applied on the agar plates were as follows: streptomycin (Sm) 200 µg/mL, neomycin (Nm) 100 µg/mL, spectinomycin (Sp) 100 µg/mL, gentamicin (Gm) 60 µg/mL. Antibiotics for *E. coli* grown on agar plate is as follows: gentamicin (Gm) 10 µg/mL, tetracycline (Tc) 5µg/mL, chloramphenicol (Cm) 5 µg/mL, rifampicin (Rf) 20 µg/mL, kanamycin (Km) 25 µg/mL. The concentration of different antibiotics in liquid media was half the concentration of the agar plate. The M9 minimum media was prepared by adding M9 (48mM disodium phosphate, 22 mM monopotassium phosphate, 8.6mM sodium chloride, 18.6 mM ammonium chloride), 1 mM MgSO<sub>4</sub>, 0.25 mM CaCl<sub>2</sub>, 0.005 µg/ml biotin, 10 ng/ml CoCl<sub>2</sub> and a specific carbon source. When preparing ammonium free M9 media, M9 salt was prepared without adding ammonium chloride. The concentration of different carbon sources was as follows: 10 mM *trans*-4-hydroxy-L-proline, 10mM *cis*-4-hydroxy-D-proline, 10 mM D-proline, 10 mM L-proline, 10 mM succinate, or 10 mM sucrose. The concentration of different nitrogen sources were as follows: 5 mM *trans*-4-hydroxy-L-proline, 5 mM *cis*-4-hydroxy-D-proline, 5 mM D-proline, 5 mM L-proline. M9 minimum agar plate was made with addition of 2X agar.

## **Transduction**

Phage lysates were made by adding 100µL of a ΦM12 phage lysate to the *S. meliloti* culture which had the OD<sub>600</sub> of 0.4. The culture-phage mixture was incubated overnight at 30°C. Non-lysenko cells were killed by adding two drops of chloroform. Lysates for transduction were diluted 1:25 with LBmc and stored at 4°C. Transduction was performed by adding 500 µL of recipient cells and 500 µL of phage lysate, which was incubated for 20 minutes at 30°C. The cells were subsequently spun down at 13,000 rpm for 1 minute and washed with 0.85% NaCl twice. 100 µL of cells were plated on selective media and 100 µL the phage lysate and recipient cell were plated as a control. The transductant colonies were streak- purified twice before being used for further experiments.

## **Conjugation**

To transfer a plasmid from a donor strain to a recipient strain, the donor and recipient strains and the helper strain carrying the mobilizing plasmid pRK600 were grown overnight. 1 mL of each strain was spun down at 13,000 rpm for 1 minute and subsequently washed with 0.85% NaCl twice. 25 µL of each washed cells were mixed and spotted on LB plate overnight at 30°C. The mating spot was resuspended in 1mL 0.85% NaCl and plated on selective media. In the meantime, donor mixed with recipient, donor mixed with helper, recipient mixed with helper, individual donor, recipient and helper, were also plated as a negative controls. The transconjugant colonies were streak-purified twice before being used for further experiment.

## Transformation

Plasmid DNA was extracted by Geneaid High-Speed Plasmid Mini Kit. 1.5-2  $\mu\text{L}$  of plasmid DNA was added to 200  $\mu\text{L}$  aliquots of DH5 $\alpha$  competent cells and kept on ice for 20 minutes. The cells were heat shocked in a 42 $^{\circ}\text{C}$  water bath for 2 minutes and then placed back on ice for 1 minute. 1 mL of LB was added to the cells and they were incubated at 37 $^{\circ}\text{C}$  with agitation for 1 hour. Afterwards, 100  $\mu\text{L}$  of the transformation mixture was plated on selective media and transformants were streak-purified twice before being used for further experiment.

## Construction of the $\Delta araE$ , $\Delta hypH$ double mutant.

*hypH* is one of the genes in hydroxyproline catabolism locus in *S.meliloti* and is annotated as putative KGSADH, which catalyzes the conversion of  $\alpha$ -KGSA to KG. However, a  $\Delta hypH$  mutant is capable grew on 4-L-Hyp, possibly due to another KGSADH enzyme from other catabolic pathway. A potential gene annotated as KGSADH is *araE* which is involved in L-arabinose catabolic pathway. A  $\Delta araE$ ,  $\Delta hypH$  double mutant was made by transducing  $\Phi\text{RmP2516}(\Delta hypH::Gm^r)$  into  $\Delta araE::Tn5$  mutant.

## Reintroducing *hypS*<sup>+</sup> into the *hypS*<sup>-</sup> mutant strain

A non-polar deletion mutant strain RmP2514 (*hypS*<sup>-</sup>) was used as the recipient. The donor strain was *E.coli* M1822, which carries the suicide plasmid pUCP30T(Gm<sup>r</sup>) with the complete *smb20261* gene and approximately 300 nt flanking each end. The functional copy of *hypS* was reintroduced by conjugation and selected on LB+Sm200+Gm60.

## Proline Auxotroph

Both the *proC* and *smb20003* genes are annotated as encoding  $\Delta^1$ -pyrroline-5-carboxylate reductase enzyme, which catalyzes the reduction from  $\Delta^1$ -pyrroline-5-carboxylate to L-proline. A proline auxotroph was constructed by mutating those two genes (G. diCenzo, unpublished). It was constructed by transduction to have a *Tn5*-B20 transposon inserted into the *proC* gene and also *smb20003* gene deleted. In the meantime, in order to test whether *hypS* is playing has a role in converting either hydroxyproline or D-proline to L-proline, a new triple mutant strain RmP3153 (*proC*,  $\Delta$  *smb20003*,  $\Delta$  *hypS*) was made by transducing the  $\Delta$ *smb20003*(*Gm<sup>r</sup>*) mutation from RmP2707 to the double mutant RmP3152(*proC*,  $\Delta$ *hypS*)

## *hyp* gene expression

To study *hyp* gene expression, transcriptional fusions to the reporter genes *lacZ* or *gusA* were used (Cowie et al., 2006b).  $\beta$ -Galactosidase activity was measured spectrophotometrically by its end product at 420nm, while  $\beta$ -Glucuronidase activity was measured spectrophotometrically by its end product at 405 nm. LacZ buffer (60 mM  $\text{Na}_2\text{HPO}_4 \cdot 7\text{H}_2\text{O}$ , 40 mM  $\text{NaH}_2\text{PO}_4$ , 10 mM KCl, 1 mM  $\text{MgSO}_4$ , 0.8 mg/ml 2-nitrophenyl- $\beta$ -D-galactopyranoside, 0.0125% SDS, and 40 mM  $\beta$ -mercaptoethanol) and GusA buffer (50 mM sodium phosphate buffer (pH 7), 1 mM EDTA, 0.44 mg/ml *p*-nitrophenyl  $\beta$ -D-glucuronide, 0.0125% SDS, and 50 mM dithiothreitol) were prepared fresh. All the cells were grown in LB with appropriate antibiotics overnight, followed by subculturing into

different M9 minimum media supplemented with various carbon sources with an initial OD<sub>600</sub> of 0.05, including 10 mM succinate, 10 mM L-proline, 10 mM D-proline or 10mM *trans*-4-hydroxy-L-proline. The cells were washed with 0.85% NaCl prior to the reaction. 20 µl culture was mixed with 80 µL LacZ or GusA buffer and incubated for 1 hour at room temperature. The reaction was terminated by adding 100 µL 1 M Na<sub>2</sub>CO<sub>3</sub>. The activity was measured at 420nm/405nm by using Molecule Devices microplate spectrophotometer. Background was also measured with 20 µL 0.85% NaCl instead of culture. The activity was calculated as follows:

$$\text{Miller Unit} = \frac{1000 \times \text{OD } 420 / \text{OD } 405}{\text{Time (min)} \times \text{Volume (mL)} \times \text{OD } 600}$$

Time (min): Reaction time

Volume: culture volume in 1 mL

## **Growth in liquid media**

Growth of different *S. meliloti* strains was measured in M9 minimum media supplemented with various carbon sources. 1 mL of cell culture was washed with 0.85% NaCl twice and resuspended in 0.85% NaCl. The cell suspension was subcultured in M9 minimum media supplemented with different carbon sources with an initial OD<sub>600</sub> of 0.05. OD<sub>600</sub> was read at every 15 minutes for 48 consecutive hours by TECAN plate reader with triplicate assays.

## **Synthesis of Δ<sup>1</sup>-pyrroline-2-carboxylate**

As Δ<sup>1</sup>-pyrroline-2-carboxylate is a potential product of the oxidation of L-proline by

HypS, we wished to determine whether HypS can reduce  $\Delta^1$ -pyrroline-2-carboxylate and simultaneously oxidize NADPH. To investigate this possibility, it was necessary to synthesize  $\Delta^1$ -pyrroline-2-carboxylate, as this compound was not commercially available.

$\Delta^1$ -Pyrroline-2-carboxylate was synthesized from D-proline in a reaction mixture containing 25 mM ammonium bicarbonate (pH 8.3), 10 mM D-proline, 0.25 mg porcine D-amino acid oxidase(DAAO) and 1000-2500 units bovine catalase in a total volume of 1mL, and the reaction was incubated overnight at 37°C and was terminated by addition of 700  $\mu$ l of ice-cold acetonitrile which denatured the protein in the reaction mixture, followed by incubation on ice for 30 minutes. The precipitate was removed by centrifugation at 13,000 rpm for 2 minutes. The supernatant, containing  $\Delta^1$ -pyrroline-2-carboxylate, was used for experiments(Visser et al., 2012b). For those  $\Delta^1$ -Pyrroline-2-carboxylate using for further reaction with HypS, no acetonitrile was added to the reaction mixture, as the solvent will denature the protein.

### **Sample preparation and direct infusion in Mass Spectrometer**

The enzymatically synthesized product  $\Delta^1$ -pyrroline-2-carboxylate was detected by mass spectrometry. The supernatant containing  $\Delta^1$ -pyrroline-2-carboxylate was diluted by HPLC grade ACN:H<sub>2</sub>O (1:1) to 100  $\mu$ M before injecting into the mass spectrometer. Both Solution A (Acetonitrile) and Solution B (H<sub>2</sub>O with 10mM Ammonium Acetate) were prepared as the running buffer. The Bruker microTOF mass spectrometer was set to ESI negative mode to detect R<sup>-</sup> group, as amino acids carry the COOH group. The samples were directly infused into the mass spectrometer with high accurate mass detection. The spectra

showed the  $m/z(M-H)$  of the compound which lost a hydrogen. That mass corresponds to the isotopic mass of the unknown compound.

### **Synthesis of $\Delta^1$ -pyrroline-4- hydroxy-2-carboxylate**

The reaction is in 1 mL mixture containing 50 mM Tris-HCl buffer (pH 9.0), 2 mM  $MgCl_2$ , 50 mM cis-4-D-Hyp, 0.05 mM PMS and 38  $\mu g$  HypO which was purified by Guia. The reaction was incubated at 30°C in the dark overnight (Watanabe et al., 2012).

### **HypS Enzymatic Assay**

The purified HypS was used to assay on different substrates. The assays of the oxidation reaction were conducted at room temperature in a 1mL cuvette with 100  $\mu L$  of various concentrations of substrate, 100  $\mu L$  of a 1 M stock solution of Tris-HCl buffer (pH 10.0), 100  $\mu L$  of a 10mM stock solution of  $NADP^+$ , 700  $\mu L$  ddH<sub>2</sub>O and 13  $\mu g$  HypS enzyme. Furthermore, the assays of the reduction reaction were conducted at room temperature in a 1 mL cuvette with 100  $\mu L$  of various concentrations of substrate, 100  $\mu L$  of a 1M stock solution of ammonium bicarbonate buffer (pH 8.3), 100  $\mu L$  of a 10 mM stock solution of NADPH, 700  $\mu L$  ddH<sub>2</sub>O and 13  $\mu g$  HypS enzyme. In the meantime, two controls were also included as the reaction mixture without HypS or substrate respectively. The product of the reaction was quantified by measuring the accumulation or the decrease of NADPH, which has absorbance change at 340 nm by using spectrophotometer. The initial rate was obtained over the first 0.2 min. The molar extinction coefficient of NADPH at 340 nm is  $6200 M^{-1} \cdot cm^{-1}$ . The Enzyme specific activity was calculated by the following equation 1.

$$\text{Enzyme specific activity } (\mu\text{mol}/\text{min}/\text{mg}) = \left( V_t * \Delta A / \Delta t \right) / \left( e * L * V_s * C_s \right) \quad \text{Eq.1}$$

V<sub>t</sub> : Reaction volume, 1 mL;

V<sub>s</sub> : Enzyme volume, 2\*10<sup>-3</sup> mL;

C<sub>s</sub> : Enzyme concentration, 6.5 mg/mL

e : The molar extinction coefficient, 6200 M<sup>-1</sup>cm<sup>-1</sup>;

L : light path (cm), 1.0 cm

ΔA/Δt: absorbance change (340nm) per minute

## Amino acid sequence alignment and phylogenetic analysis

Amino acid sequences of the New family of NAD(P)H-dependent oxidoreductases were taken from NCBI data banks (Muramatsu et al., 2005a; Muramatsu et al., 2005b). Multiple amino acid sequence alignment and the phylogenetic tree were created by using MAGA6 (Tamura et al., 2013).

## Determine the concentration of α-KGSA stock solution

The concentration of the α-KGSA in the resulting stock solution was determined enzymatically using α-KGSA dehydrogenase and allowing the reaction to proceed to completion ( $\alpha\text{-KGSA} + \text{NADP}^+ \rightleftharpoons \alpha\text{-KG} + \text{NADPH} + \text{H}^+$ ). Assuming an NADPH:KG ratio of 1:1 and that the reaction resulted in 100% conversion of α-KGSA when NADP was present in excess. The reaction was carried out for an hour in 1 mL volume with 5 μL α-KGSA stock solution and 0.5 mM NADP<sup>+</sup> in 50mM HEPES buffer (pH 7.5) with 100 mM NaCl and 0.5 mM MgCl<sub>2</sub>, with addition of 2.36μg HypH enzyme. The reaction was completed and the final

concentration of  $\alpha$ -KGSA was calculated as 2.23 mM.

### **12% SDS Polyacrylamide Gel Electrophoresis**

SDS-PAGE gel contained 12% Bis-acrylamide and the stacking and resolving gels were prepared as previously described (Sambrook 2001). 1 mL of overnight cell culture was spun down and resuspended in 100  $\mu$ l 1X SDS loading dye prior to boiling for 5 minutes to lyse the cells. The lysed cells were centrifuged for 5 minutes at 13,000 rpm. 4  $\mu$ l of the supernatant from each sample was loaded and run at 150 V until the loading dye reached the bottom of the gel.

### **BL21/DE3 pLysS competent cell**

*E.coli* J618 (BL21/DE3 pLysS) competent cells were made by using  $\text{CaCl}_2$ . The J618 colonies were inoculated in LB overnight. Next morning the cells were subcultured in 100 mL LB with an initial  $\text{OD}_{600}$  of 0.05 and grown until an  $\text{OD}_{600}$  of 0.4. The cultures were cooled on ice for 10 minutes. Afterwards, the culture were spun down at 4,400 rpm at 4°C for 10 minutes. The cell pellets were resuspended with 25 mL 100 mM  $\text{CaCl}_2$  solution and kept on ice for 30 minutes. After that, the culture was centrifuged and resuspended in 3 mL 100 mM  $\text{CaCl}_2$ +15% glycerol. Finally each of 30 micro tubes was filled with 200  $\mu$ L cells and frozen immediately in liquid nitrogen. The competent cells were store in “Sharon” box in -80°C freezer on the fifth floor

## Purification of HypD

A vector pTH2721 which carries *smb20259* cloned into pET28a for over-expression with an N-terminal His6 tag, as well as kanamycin resistance, was saved in *E.coli* DH5 $\alpha$  cells (M1859). *smb20259* in pET28a was transcribed from T7 promoter in the presence of a T7 RNA polymerase. The plasmid was extracted from the DH5 $\alpha$  cells by using the Presto Mini Plasmid Kit. Afterwards the plasmid was transformed into BL21/DE3 pLysS competent cells for over expression. The transformants were selected on LB+Km25.

The colonies of BL21/DE3 pLysS cells carrying the plasmid pTH2721 were inoculated in 20 mL LB+ Km<sup>25</sup> and agitated overnight at 37°C, followed by subculturing in 1 L media to an OD of 0.4. The over-expression of this recombinant protein was induced by adding 0.5 mM IPTG. The culture was incubated with agitation for 4 hours at 30°C. Afterwards the cells were spun down at 4°C for 20 minutes at 16,000 RCF, followed by suspension in a ice cold buffer to a final volume of 30 mL, containing 50 mM Tris-HCl (pH8), 150 mM NaCl and 7.5% glycerol. The whole cells were passed through a 40K French Pressure cell six times at 1280 psi. The total lysate was centrifuged at 4°C for 45 minutes at 24,000 RCF by using Beckman Avanti J-25 centrifuge (JA-20 rotor, 24,000 RCF). The cytoplasmic protein HypD protein was in the supernatant.

A 8 mL TALON Metal Affinity Resin Co<sup>2+</sup> column was packed to purify the His-tag HypD protein. The resin was equilibrated with 10 bed volume of equilibration buffer containing 50 mM Na-phosphate (pH 7.0), 300 mM NaCl and 20 mM imidazole (pH 7.0). The 25 mL of supernatant was loaded onto the column twice and washed with 10 bed volumes of wash buffer to remove unspecific binding protein. The remaining proteins were eluted with 50

mM Na-phosphate (pH 7.0), 300 mM NaCl and 200 mM imidazole (pH 7.0). 60 fractions were collected in 500  $\mu$ L quantities. After protein elution, the resin should be regenerated by 0.2 M EDTA (pH 7.0) and 50 mM  $\text{CoCl}_2$  prior to store at 4  $^\circ\text{C}$  for long term usage.

The protein concentration of each fraction was determined by using the Bio-Rad assay compared with the BSA standard curve. The assay was carried out by adding 5  $\mu$ L protein of each fraction to 200  $\mu$ L Bio-Rad dye reagent and 800  $\mu$ L ddH<sub>2</sub>O. The highest concentration of fractions were pooled into six fractions. A 12% SDS-PAGE gel was run to analyze the six fractions against uninduced cell, uninduced whole cell, total lysate, supernatant, flow through and wash.

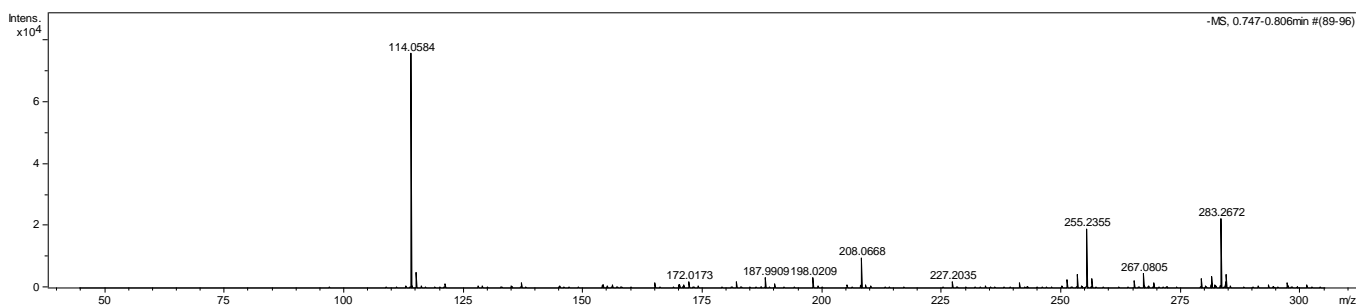
The six fractions with the highest concentration of protein were loaded on a 5 mL Amersham HiTrap desalting column running on the FPLC system to change the storage buffer containing 20 mM HEPES (pH 7.5), 150 mM KCl, 1 mM DTT, 1 mM EDTA, 10% glycerol. The six fractions were then pooled and concentrated by using Pall 10K mega Microsep Advance Centrifugal Devices, which were centrifuged at 10,860 RCF for 15 minutes at 4  $^\circ\text{C}$ . The final concentration of the protein was 6.28 mg/mL. In total, 40.19 mg of total proteins were aliquots at -80  $^\circ\text{C}$ .

## RESULTS

### Enzymatic synthesis of $\Delta^1$ -pyrroline-2-carboxylate

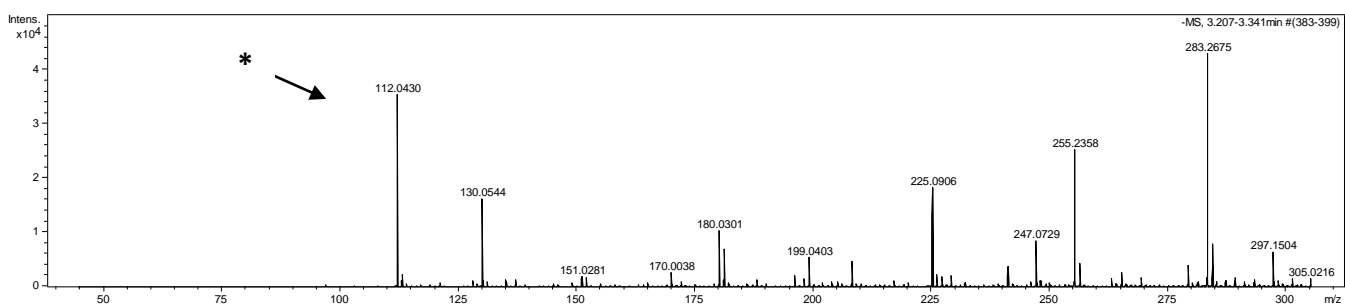
As HypS appeared to catalyze the NADP-dependent oxidation of L-proline to  $\Delta^1$ -pyrroline-2-carboxylate, we wished to investigate whether HypS would catalyze the reduction of  $\Delta^1$ -pyrroline-2-carboxylate. As  $\Delta^1$ -pyrroline-2-carboxylate is not commercially available, we sought to synthesize it from D-proline using the enzyme D-amino acid oxidase (DAAO) (Visser et al., 2012a). Reaction mixtures containing D-proline, DAAO and catalase were incubated at room temperature for 24 hours. To investigate the product made in this reaction, the reaction mixture diluted (1:25) with acetonitrile:H<sub>2</sub>O (1:1) was directly infused into and monitored by mass spectrometry in ESI-negative mode. The mass scan was set in the range m/z=0-300. In a control reaction mixture containing D-proline without DAAO and catalase, a peak was observed at m/z=114 that corresponded to D-proline (Figure 4A). Following 24 hours incubation in the presence of both enzymes, a new peak was observed at m/z=112, which was the expected product  $\Delta^1$ -pyrroline-2-carboxylate (Figure 4B). Noticeably, a second peak at m/z=130 was observed and this was absent in the control. This implied that an open form  $\alpha$ -keto- $\delta$ -aminovalerate might coexist with  $\Delta^1$ -pyrroline-2-carboxylate. As shown in Figure 4, D-proline was about fully converted to  $\Delta^1$ -pyrroline-2-carboxylate and this preparation was used when  $\Delta^1$ -pyrroline-2-carboxylate was required for further reactions with the enzyme HypS. No D-proline was detected in the reaction mixture.

A)



T=0

B)



T=24 hrs

**Figure 4.** Identification of the product of D-proline by DAAO. A) mass spectra of a reaction mixture without DAAO and catalase at time zero. B) After reaction for 24 hrs, a newly formed peak at m/z 112 is marked with an asterisk. D-proline have m/z 114. Another prominent peak at m/z 130 might be an open form  $\alpha$ -keto- $\delta$ -aminovalerate. D-proline m/z (M-H)=114.06,  $\Delta^1$ -Pyrroline-2-carboxylate m/z(M-H)=112.04 (marked with an asterisk)  $\alpha$ -keto- $\delta$ -aminovalerate m/z(M-H)=130.058

### $\Delta^1$ -pyrroline-2-carboxylate reduction by purified HypS

Since DAAO appeared to fully convert D-proline to  $\Delta^1$ -pyrroline-2-carboxylate, 100  $\mu$ L aliquots from the pyrroline reaction mixture in 25 mM ammonium bicarbonate buffer, was added to 1mM NADPH and 6.5  $\mu$ g HypS in a 1 mL final volume reaction. DAAO and catalase from the pyrroline reaction mixture were still present. The enzyme activity catalyzed by HypS was measured by monitoring the reduction of NADPH. The enzyme reaction was

started by mixing the  $\Delta^1$ -Pyrroline-2-carboxylate sample, NADPH and ammonium bicarbonate buffer in a 1 mL reaction mixture in a 1 cm path-length cuvette. The concentration of  $\Delta^1$ -Pyrroline-2-carboxylate was estimated to be 1 mM, as it was fully converted from D-proline and 10 fold diluted in this reaction. The HypS protein was then added with gentle mixing. This mixture was placed into a spectrophotometer and the absorbance at 340nm was monitored for 2 min. NADPH, is the only molecule in the reaction that absorbs at 340nm and therefore, as NADPH was oxidized, the absorbance at 340nm decreased. This revealed that HypS catalyzed a  $\Delta^1$ -pyrroline-2-carboxylate-dependent oxidation of NADPH.

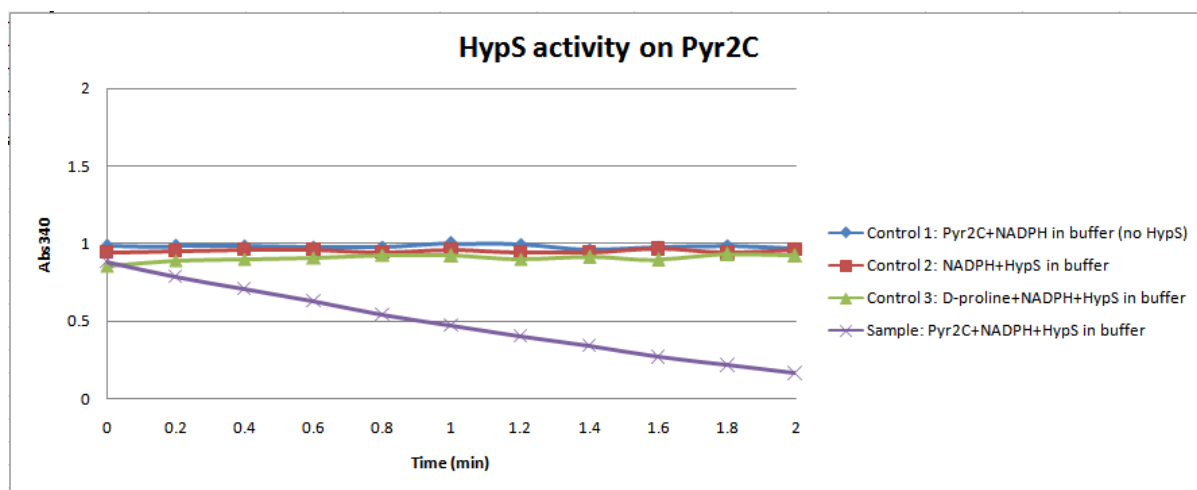


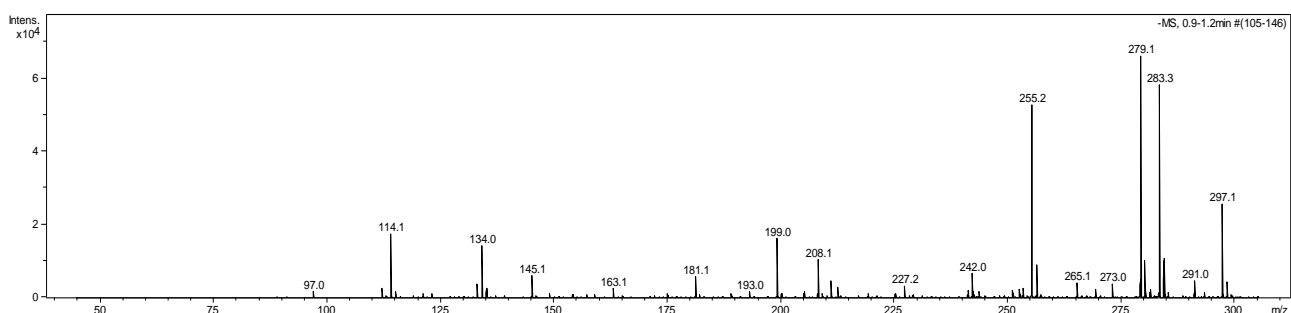
**Figure 5.** Relationship between absorbance and time following addition of 6.5  $\mu$ g HypS to a 1 ml final volume reaction mixture containing 1 mM NADPH, 25 mM ammonium bicarbonate (pH 8.3) and 1 mM of  $\Delta^1$ -pyrroline-2-carboxylate (1:10 dilution of the D-proline, DAAO reaction mixture) .

### Products formed from the HypS and NADPH-dependent reduction of $\Delta^1$ -pyrroline-2-carboxylate

The result shown in Figure 5 confirmed that HypS oxidized NADPH in the presence of  $\Delta^1$ -pyrroline-2-carboxylate, The products of this reaction were analyzed by mass spectrometry. The reaction occurred in a volume of 1 mL containing 100  $\mu$ L pyrroline sample

and 1 mM NADPH in ammonium bicarbonate buffer (pH 8.3) and was incubated at room temperature overnight. After that, 500  $\mu$ L acetonitrile was added to 500  $\mu$ L reaction mixture to terminate the reaction. After 13,000 rpm centrifugation for 2 minutes, the diluted supernatant was directly infused into the Bruker MicroTOF mass spectrometry. The new peak was observed at  $m/z=114$ , which was expected to be proline.

A)



B)

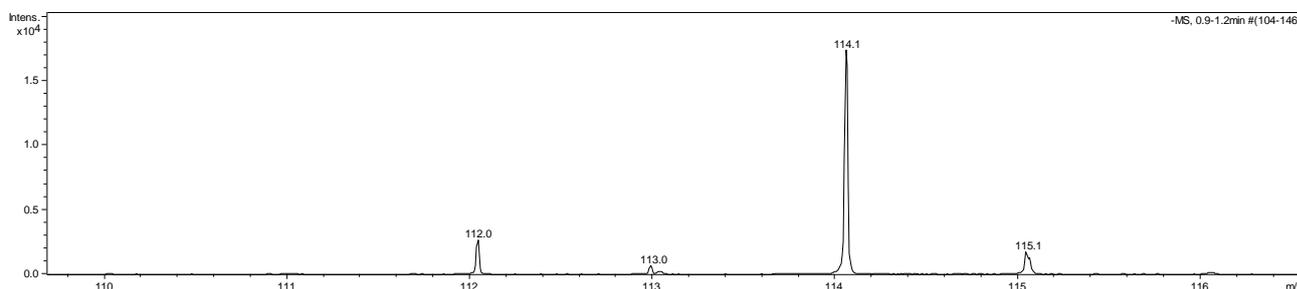


**Figure 6.** Identification of the product of pyrroline-2-carboxylate by HypS. After reaction for 24 hrs, a newly formed peak at  $m/z$  114, which is a proline product. A)  $m/z$  from 0-300. B)  $m/z$  from 110-116.

### Substrate of HypS (Oxidation)

The ability of HypS to oxidize the substrates L-proline, D-proline, L-malate, *trans*-4-hydroxy-L-proline, and *cis*-4-hydroxy-D-proline was assayed in reaction mixtures that contained 100 mM substrate, 12  $\mu$ g HypS and 1mM NADP<sup>+</sup>. The result is summarized in Table 2. The enzyme exhibited significant oxidation activity towards L-proline and also a

weak oxidation activity towards *trans*-4-hydroxy-L-proline. However, D-proline, L-malate, *cis*-4-hydroxy-D-proline did not serve as a substrate.

Substrate	S.A. ( $\mu\text{mol}/\text{min}/\text{mg}$ )
L-Proline	7.7 $\pm$ 0.3
D-Proline	0.01 $\pm$ 0.01
L-Malate	0.01 $\pm$ 0.01
<i>Trans</i> -4-L-Hyp	0.15 $\pm$ 0.01
<i>Cis</i> -4-D-Hyp	0.01 $\pm$ 0.03

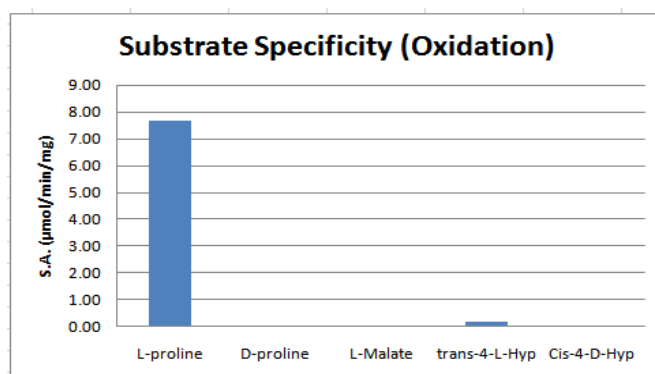


**Table 2.** Substrate specificity. Determined with 100 mM substrate and 1 mM NADP<sup>+</sup> in 100 mM Tris-HCl buffer (pH 10.0)

## Cofactor

To determine the cofactor specificity of HypS both the diphosphopyridine nucleotide and triphosphopyridine nucleotide cofactors were employed for the reduction and oxidation reactions catalyzed by HypS. 0.5 mM cofactor concentration was employed with 0.5 mM Pyr2C and 1mM for 100mM L-proline (Table 3). The data in Table 3 showed that HypS has a clear preference for the triphosphopyridine nucleotide cofactor NADP<sup>+</sup>/NADPH.

**Table 3 Specificity of HypS for phosphopyridine nucleotide cofactors**

Cofactor	S.A. ( $\mu\text{mol}/\text{min}/\text{mg}$ )
NADH <sup>a</sup>	0.45 $\pm$ 0.09
NADPH <sup>a</sup>	17.66 $\pm$ 0.12
NAD <sup>+b</sup>	0.16 $\pm$ 0.05
NADP <sup>+b</sup>	7.51 $\pm$ 0.46

<sup>a</sup> Determined with 0.5 mM Pyr2C and 0.5 mM cofactor.

<sup>b</sup> Determined with 100 mM L-Proline and 1 mM cofactor.

## Kinetics Analysis of HypS

The kinetics of the HypS catalyzed reduction of  $\Delta^1$ -pyrroline-2-carboxylate (Pyr2C) was measured at varying concentrations of Pyr2C and a constant NADPH concentration of 0.5 mM. Pyr2C concentrations exceeding 1.1 mM, there was a decrease in the rate of reaction. This was judged by analyzing the data to the hyperbolic Michaelis-Menten equation with a software Origin 8.0. The obvious substrate inhibition constant ( $K_i$ ) for Pyr2C was determined by fitting the data to equation 2.  $K_b$  represented the Michaelis constant for Pyr2C. In the non-linear regression analysis, the coefficient of curve fitting  $R^2$  was 0.9529 to the uncompetitive inhibition equation (Eq.2), which caused  $V_{max}$  and  $K_m$  decrease by its substrate inhibition (Muramatsu et al., 2005c).

$$v=V*[S]/(K_b+[S]+[S]^2/K_i) \quad \text{Eq.2}$$

The kinetics of the HypS catalyzed oxidation of L-proline were carried out at a fixed  $\text{NADP}^+$  concentration of 1 mM, and varying L-proline concentrations. The reactions were run at room temperature by adding 13  $\mu\text{g}$  HypS enzyme in 100 mM Tris-HCl buffer (pH 10.0). The product of the reaction was quantified by measuring the formation of NADPH.

The velocity of the reaction was plotted against the substrate concentration. The kinetic parameters were calculated by plotting the data to the Michaelis-Menten equation 3. with Origin 8.0 as shown in (Fig 7B). The coefficient of curve fitting  $R^2$  was 0.99572.

$$v=V_{max}*[S]/(K_m+[S]) \quad \text{Eq.3}$$

The kinetic parameters are shown in Table 4. The enzyme efficiency ( $K_{cat}/K_m$ ) of HypS with Pyr2C as substrate (2914) is distinctly larger than for L-proline (0.88) which indicates more rapid conversion from Pyr2C to L-proline than the reversed reaction. It can be also explained by the  $K_m$  and  $V_{max}$  value. 74mM L-proline is needed to reach its half maximum velocity in the oxidation reaction, while 0.27 mM Pyr2C was required in the reduction reaction. Compared to other HypS-like proteins in different organisms, the *S. meliloti*  $K_m$  value of Pyr2C (0.27) was similar to those in *A. brasilense* (0.63) and *P. aeruginosa* (0.45), while it was about twenty times smaller than that in *C. psychrerythraea* (5.90) (Watanabe et al., 2014). The smaller  $K_m$  value, the greater is the affinity of the enzyme for the substrate Pyr2C.

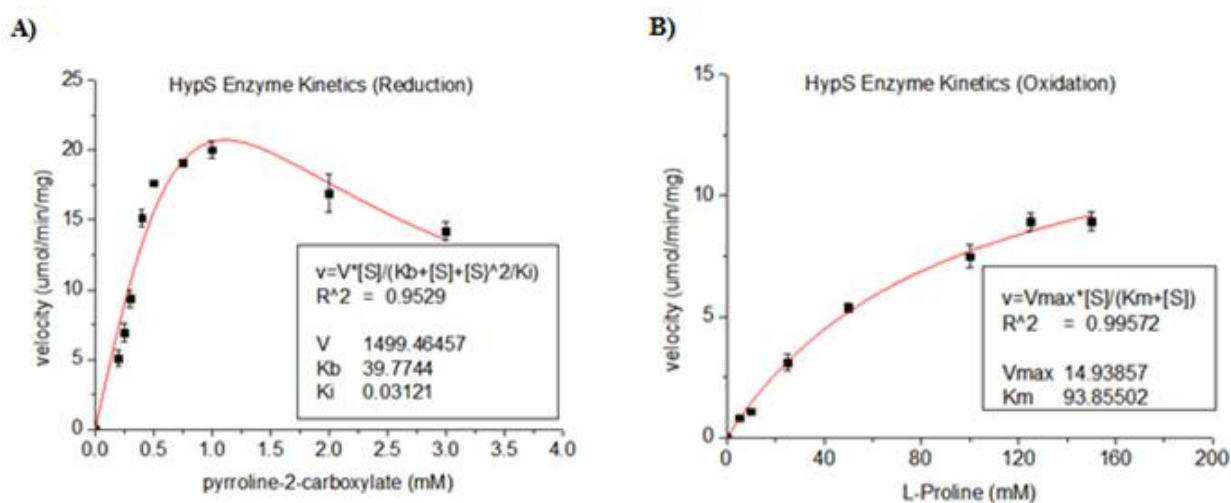


**Figure 7. HypS enzyme kinetics** A) The Pyr2C concentration varied with a fixed concentration of NADPH at 0.5mM. The data was plotted by using non-linear regression fitting by using equation 2. B) The L-proline concentration varied with a fixed concentration of  $\text{NADP}^+$  at 1mM. The data was plotted by using non-linear regression fitting by using equation 3. The reactions were run at room temperature and contained 13  $\mu\text{g}$  HypS protein in 25 mM ammonium bicarbonate buffer (pH 8.3) or 100 mM Tris-HCl (pH 10.0) in a final volume of 1 mL.

**Table 4.** Kinetic parameters of HypS in the reduction and oxidation reaction

	Pyr2C	L-proline
Vmax ( $\mu\text{mol}/\text{min}/\text{mg}$ )	20.7	1.71
Km (mM)	0.27	74.03
Ki (mM)	0.03	-
Kcat ( $\text{min}^{-1}$ )	786.8	65.0
Kcat/Km ( $\text{mM}^{-1}\text{min}^{-1}$ )	2914.1	0.88

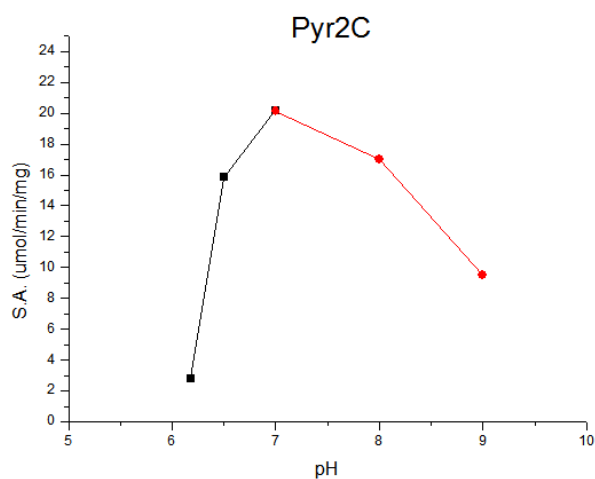
※Since M-M equation  $v=1499.5[S]/(39.8+[S]+[S]^2/0.03)$ , when  $[S]=(K_b \cdot K_i)^{1/2}=1.114$  mM, v reaches the highest value  $V_{\text{max}}=V/(2 \cdot (K_b/K_i)^{1/2}+1)=20.7$   $\mu\text{mol}/\text{min}/\text{mg}$ .

※ $K_{\text{cat}}=V_{\text{max}}/[E]$ . Where MW of HypS is 345aa=345\*110=37.95kDa, so the concentration of the enzyme is  $6.5\text{mg}/\text{mL}=6.5/37.95 \cdot 10^3=0.171\text{mM}$ .  $[E]=0.342\mu\text{M}$   $V_{\text{max}}=20.7\mu\text{mol}/\text{min}/\text{mg}=0.2691\text{mM}/\text{min}$ . Therefore,  $K_{\text{cat}}=V_{\text{max}}/[E]=786.8/\text{min}$

## pH effect

To determine the optimum pH for HypS, the reduction and oxidation reactions were performed at various pH values. As shown in Fig.8, the optimum pH for the HypS reduction of Pyr2C was pH 7.0, whereas the optimum pH for the oxidation of L-proline occurred at pH 10.0.

A)



B)

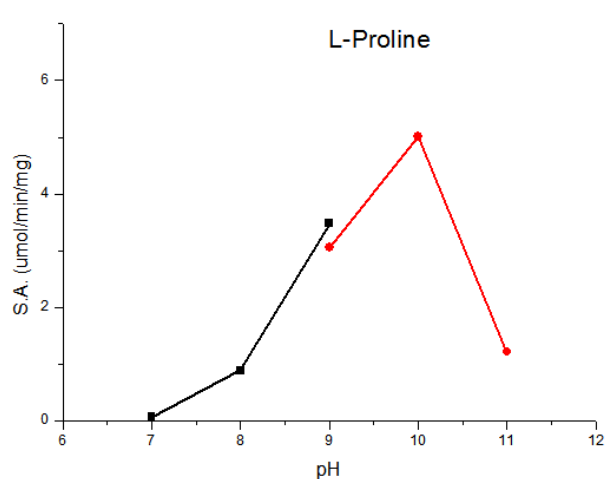


**Figure 8. pH effect on the activity of HypS.** A) The reduction of Pyr2C. The assay was carried out with 100mM PIPES buffer (pH 6.18-7.0) and 100mM Tris-HCl buffer (pH 7.0-9.0). B) The oxidation of L-Proline. The assay was carried out with 100mM Tris-HCl buffer (pH 7.0-9.0) and 100 mM Glycine-NaOH buffer (pH 9.0-11.0)

## ***hypS* is involved in D-proline metabolism**

### **Growth of a $\Delta hypS$ mutant on D-proline**

A *hypS* deletion mutant, RmP2514 in which *hypS* was replaced by an FRT scar sequence was previously constructed by Catharine White (White and Finan unpublished). This non-polar *hypS* deletion mutant was made in the wild type RmP110 background. To evaluate any phenotypes that result from the  $\Delta hypS$  mutation, we reintroduced the wild type *hypS* gene into RmP2514 background (see Figure 9). This was accomplished by integrating a suicide plasmid (pUCP30T) that carried *hypS* and ~ 300 nt of flanking sequence (pTH2685) into the RmP2514 strain as schematically outlined in Figure 9 and the Materials and Methods. The mutant strain was tested for growth on D-proline as the sole source of carbon or nitrogen, or the sole source of carbon and nitrogen. The  $\Delta hypS$  mutant, RmP2514, its *hypS*<sup>+</sup> derivative, strain RmP3272 (RmP2514::pTH2685), and strains RmP3155 ( $\Delta smb20003$ , *proC*), RmP3153 ( $\Delta smb20003$ , *proC*,  $\Delta hypS$ ) and RmP110 (wild type) were tested for growth on D-proline as the sole source of carbon or nitrogen, or the sole source of carbon and nitrogen. The results were summarized in Table 5 and Appendix Figure 28.

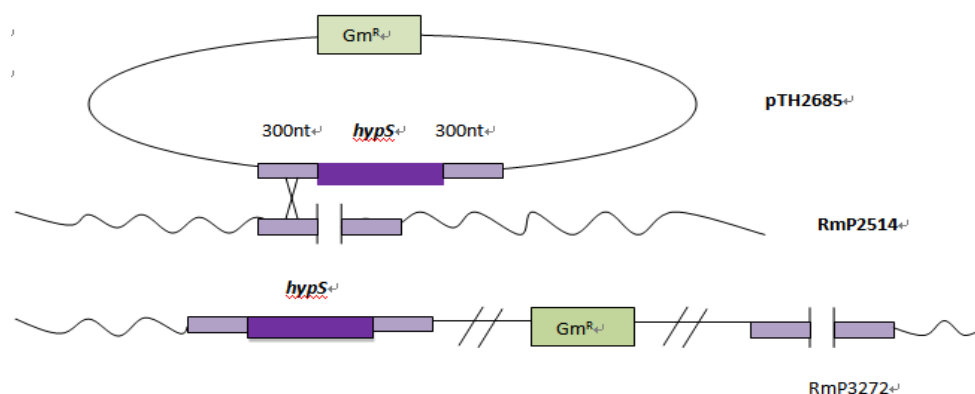


**Figure 9. Schematic of *hypS* gene reintroducing into *hypS* mutant strain.** Suicide plasmid pTH2685 carries *hypS* gene and gentamicin resistance. The transconjugants were selected on Sm200+Gm60.

**Table 5. Growth of *S. meliloti* on Minimum Agar plate with various sources of carbon and nitrogen**

Strain	L-proline as sole source of carbon <sup>a</sup>	D-proline as sole source of carbon <sup>b</sup>	D-proline as sole source of nitrogen <sup>c</sup>	D-proline as sole source of carbon and nitrogen <sup>d</sup>
RmP110 (WT)	+++++	+++	+++	++
RmP2514 ( $\Delta hypS$ )	+++++	-	-	-
RmP3155( $\Delta smb20003, proC$ )	+++++	+++	+++	++
RmP3153( $\Delta smb20003, proC, \Delta hypS$ )	+++++	-	-	-
RmP3272 (RmP2514 (pTH2685))	+++++	+++	+++	++

a – L-proline concentration is 10mM

b - D-proline concentration is 10 mM

c - D-proline concentration is 2 mM, 10 mM sucrose as carbon source. Nitrogen free M9 salt was made lacking  $NH_4Cl$ .

d – D-proline concentration is 10 mM. Nitrogen free M9 salt was made lacking  $NH_4Cl$ .

The “+”, “-” symbol showed in the table indicate the colony size

“+++++” – Large

“+++” – Medium

“++” – Smaller than medium

“-” – Not grow

The results showed that the  $\Delta hypS$  mutant was not capable of growth on D-proline as the carbon or nitrogen source. Moreover, D-proline also alleviated the auxotrophic requirement of the  $\Delta smb20003, proC$  double mutant for L-proline. That revealed that *hypS* was involved in the metabolism of D-proline to synthesize L-proline, which rescued the

L-proline auxotrophy. These growth data are consistent with the biochemical data showing that the HypS protein can reduce  $\Delta^1$ -pyrroline-2-carboxylate to L-proline. The catabolic pathway for D-proline therefore appears to involve the conversion of D-proline to  $\Delta^1$ -pyrroline-2-carboxylate and its subsequent conversion to L-proline by HypS. The transporter(s) involved in the uptake of D-proline and its oxidation to  $\Delta^1$ -pyrroline-2-carboxylate remain to be identified.

#### **Growth of *ΔhypS* mutant in liquid media.**

The ability of the *ΔhypS* mutants to grow in liquid M9 minimum media with 10mM L-proline, or 10mM D-proline, or 10mM L-Hydroxyproline as the sole source of carbon was examined (Figure 10). In addition, the wild type RmP110, and mutant strains RmP3155 (*proC*, *Δsmb20003*), and RmP3153 (*proC*, *Δsmb20003*, *ΔhypS*), and the complemented strain RmP3272 (RmP2514(pTH2685)) were also examined. All the strains grew as well as the wild type strain when L-proline was the sole carbon source. D-proline served as the sole carbon source for the wild type, RmP110, although there was a longer lag phase with D-proline than with L-proline as carbon sources. The proline auxotroph RmP3155 and complemented strain RmP3272 exhibited a long lag and started to grow after 30 hours. Both the *ΔhypS* mutant RmP2514 and RmP3153 failed to grow with D-proline, while both these strains grew with L-proline as carbon source. In media with L-hydroxyproline as carbon source, both RmP3155 and RmP3153 grew more poorly than wild type. That was probably due to minor L-proline present in L-hydroxyproline stock solution.

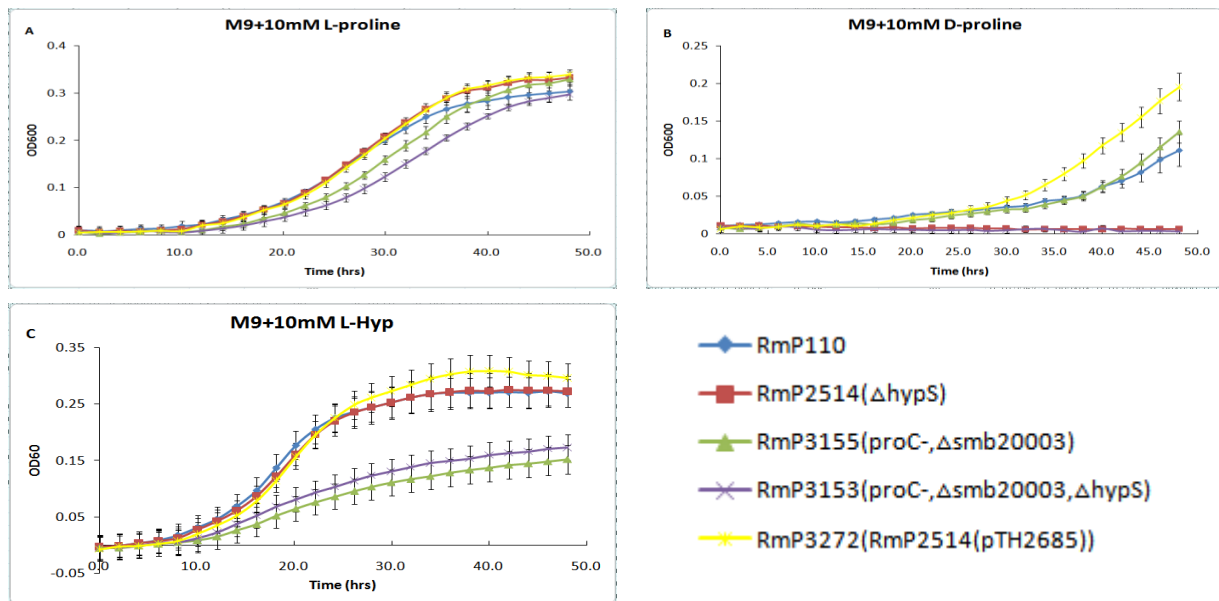


**Figure 10.** Growth curve of different  $\Delta hypS$  mutant in M9 minimum media supplemented with various carbon source.

### ***hyp* genes expression**

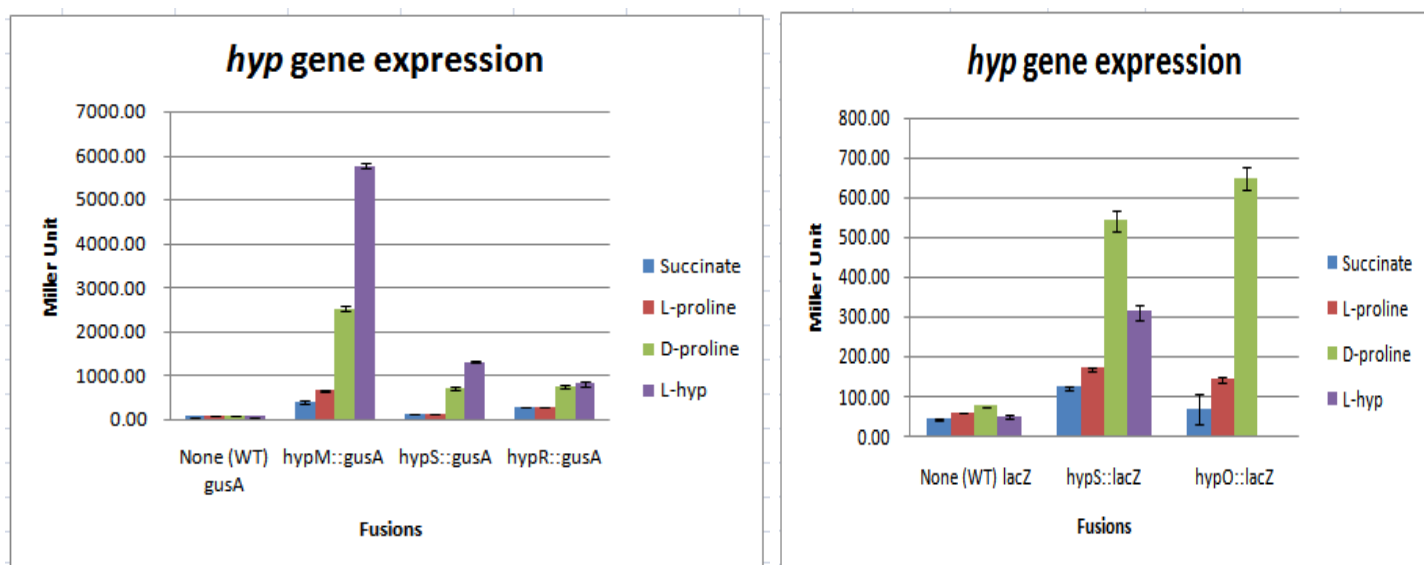
To study the *hyp* gene expression, transcriptional fusions to the reporter genes *gusA* or *lacZ* were used (Cowie et al., 2006a; Cowie et al., 2006b). Assays were conducted with cells grown on 10 mM succinate, L-Hyp, L-proline or D-proline as the carbon source. All the fusion strains were subcultured to an initial OD<sub>600</sub> of 0.05 and were grown for 40 hours in M9 minimum media supplemented with various carbon sources and the results are summarized in Table 6. Strain RmP2551 did not grow in L-Hyp, as the *hypRE* gene was disrupted in this fusion strain. The data showed, that the *hyp* genes were slightly induced in cells growing with D-proline compared to L-Hyp. However, the induction was somehow higher than with L-proline and succinate.

**Table 6.** *hyp* genes expression

Strain	fusion	Succinate	L-proline	D-proline	L-hyp
RmP110	None (WT) <i>gusA</i>	41.89±2.09	43.14±1.12	39.75±1.88	34.63±1.72
RmP1886	<i>hypM::gusA</i>	496.37±23.77	863.70±28.77	1220.50±1.65	1296.58±28.02
RmP239	<i>hypS::gusA</i>	88.90±0.46	120.50±1.54	184.32±3.03	1029.70±8.11
RmFL2315	<i>hypR::gusA</i>	249.96±10.80	205.92±10.14	365.25±13.51	615.89±41.98
RmP110	None (WT) <i>lacZ</i>	41.96±2.77	58.77±1.29	73.87±1.30	48.88±4.25
RmFL866	<i>hypS::lacZ</i>	121.83±3.91	169.20±6.16	541.11±26.44	311.98±19.01
RmP2551	<i>hypO::lacZ</i>	68.50±39.92	140.89±6.67	649.85±28.92	ND

The fusion strains were grown in M9 minimum medium with 10mM succinate, L-proline, D-proline or L-Hyp. Assays were performed in triplicate (from three different cultures). Data shown are averages with standard deviation.

ND – Not determined



## *putA*<sup>-</sup> mutant

We hypothesized that catabolic pathway for D-proline requires its conversion to L-proline and subsequent metabolism via the L-proline catabolic pathway. The L-proline utilization gene, *putA*, encodes a single bifunctional polypeptide with proline dehydrogenase and  $\Delta^1$ -pyrroline-5-carboxylate dehydrogenase activities that catalyze the conversion of L-proline to glutamate (Ostrovsky de Spicer and Maloy, 1993). A search of the reporter gene fusion library (Cowie *et al.*, 2006) identified a *putA*<sup>-</sup> mutant strain, RmFL5502. The ability of this *putA* mutant to grow with various carbon sources, including D-proline, was examined.

When L-proline was the sole carbon source, the *putA*<sup>-</sup> mutant did not grow although slight growth was observed after 50 hours. This was possibly a result of revertant *putA*<sup>+</sup> cells as the *putA*<sup>-</sup> mutation was a result of a single cross-over recombination event. When D-proline was the carbon source, the *putA*<sup>-</sup> mutant also failed to grow and thus this result is consistent with the suggestion that the D-proline catabolic pathway requires its conversion L-proline. As expected the wild-type *S. meliloti* RmP110 grew with L-proline or D-proline as carbon sources and both the wild type and *putA* mutant grew with L-hydroxyproline as the carbon source. However, *putA* mutant showed a growth lag in L-hydroxyproline compared to wild type strain. This might contribute to that *putA* mutant constitutively expressed.

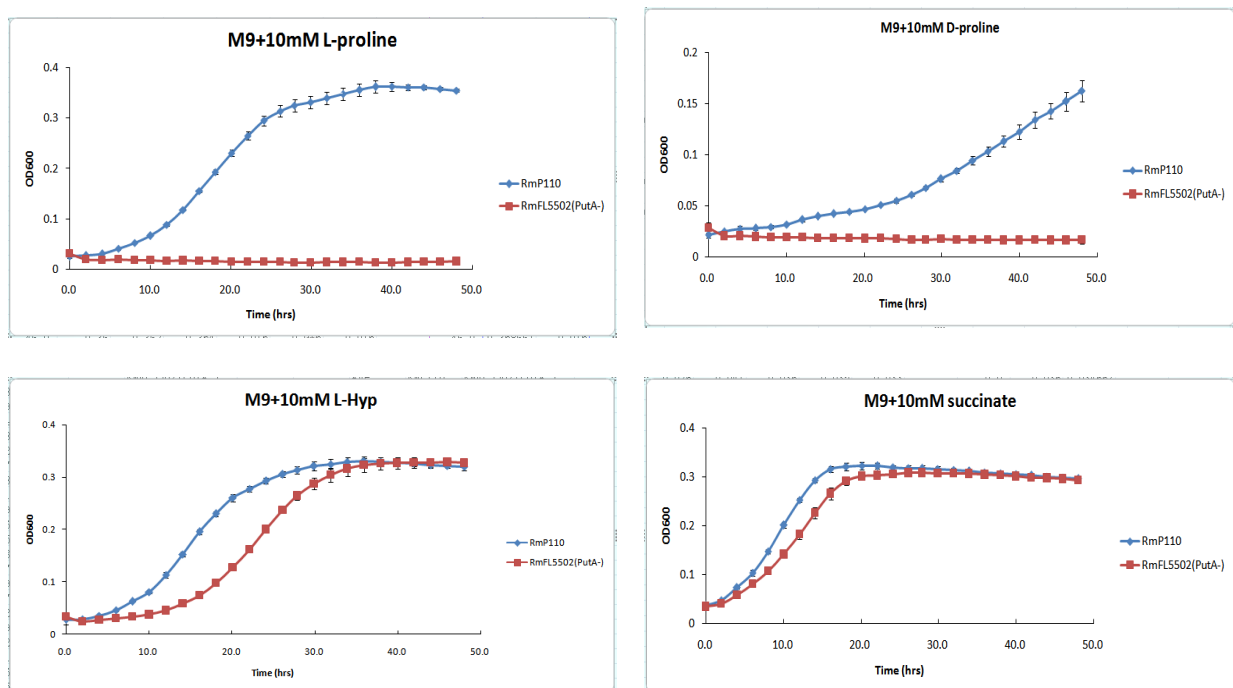


**Figure 11.** Grow of the *putA*<sup>-</sup> mutant RmFL5502 and the wild type RmP110 in M9 minimum media supplemented with D-proline, L-proline, L-hydroxyproline or succinate as carbon sources.

## How is D-proline transported into the cells

Previously *hypMNPQ* genes were reported as an ABC transporter system for the hydroxyproline uptake in *S. meliloti*. It was suggested there was a second mechanism for hydroxyproline uptake in *S. meliloti* that was induced by L-proline. Therefore, when hydroxyproline was present as the sole carbon source, the *hypMNPQ* mutant strain RmP1114 exhibited a lag in growth (MacLean et al., 2009b). In addition, The possibility that L-proline and *trans*-4-L-Hyp may share the uptake system has been raised in *P. aeruginosa* (Manoharan, 1980).

As D-proline might use the hydroxyproline or proline transport systems to be utilized by the cells, the ability of a  $\Delta$ *hypMNPQ* mutant RmP114 to grow in M9 minimum media with D-proline, L-proline and L-hydroxyproline was examined. Interestingly the  $\Delta$ *hypMNPQ* mutant grew poorly on D-proline, and L-hydroxyproline relative to L-proline and thus it appears that the *HypMNPQ* genes can facilitate D-proline uptake. We note that the *hypMPPQ* genes are induced upon growth with D-proline (see below Fig 12).

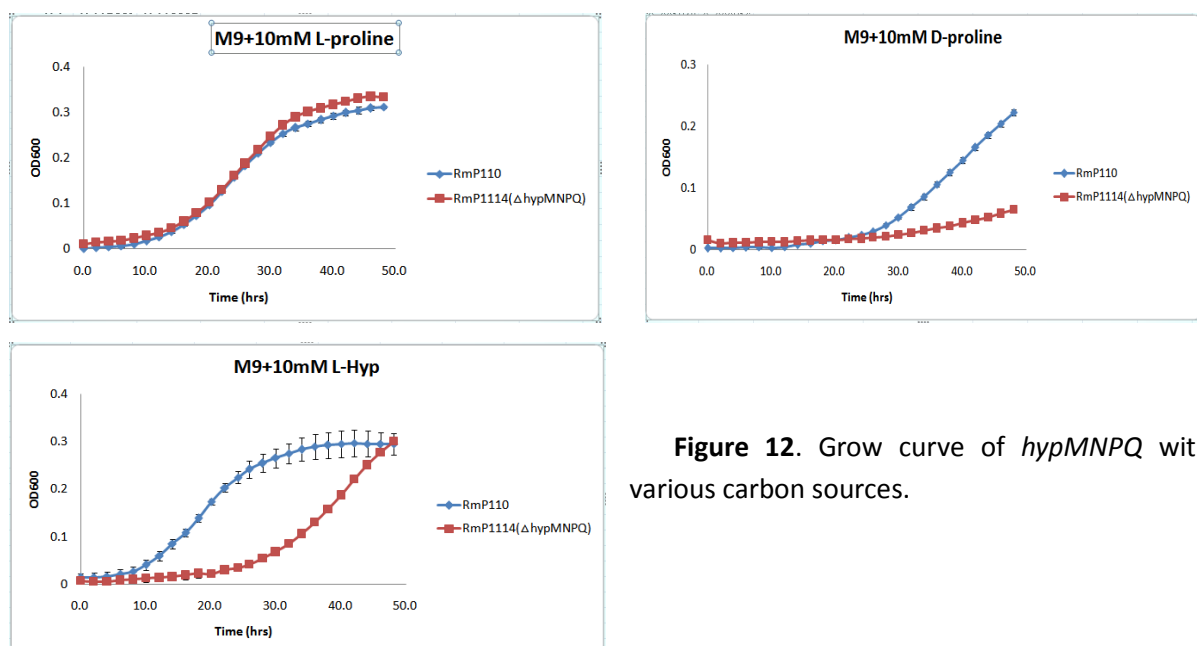


**Figure 12.** Grow curve of *hypMNPQ* with various carbon sources.

## Are other *hyp* genes involved in D-proline catabolism

Since *hypO*, *hypRE*, *hypD* genes have been characterized in the hydroxyproline catabolic pathway,  $\Delta hypO$ ,  $\Delta hypRE$ ,  $\Delta hypD$  mutants were also tested to determine if they were required in the catabolism of D-proline. Of the three mutants, only the  $\Delta hypO$  strain showed a major reduction in growth on D-proline. These data suggest that upon transport into the cell via the HypMNPQ transporter, D-proline is oxidized to  $\Delta^1$ -pyrroline-2-carboxylate by the HypO (D-amino acid oxidase) protein. As expected, the  $\Delta hypRE$  and  $\Delta hypD$  mutants did not grow with L-Hyp (White et al., 2012b) whereas both grew with D-proline. However, there are other oxidases in the cell functioning the same as HypO.

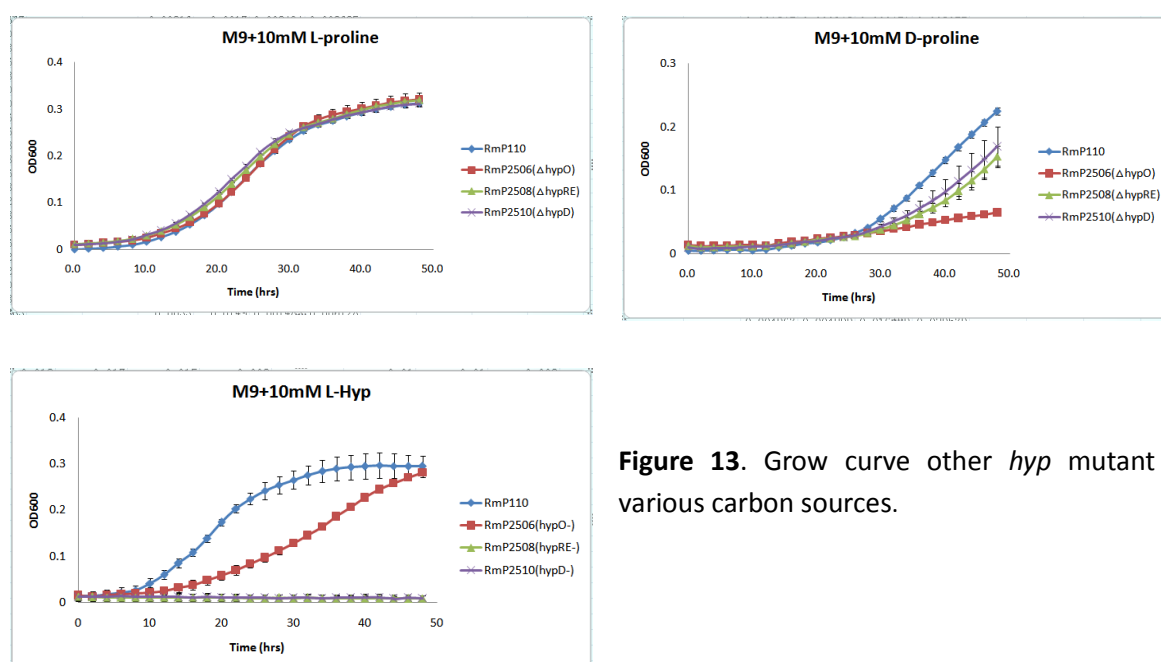


**Figure 13.** Grow curve other *hyp* mutant with various carbon sources.

## HypS can also reduce $\Delta^1$ -Piperidine-2-carboxylate

$\Delta^1$ -Piperidine-2-carboxylate was synthesized from D-lysine in a reaction mixture containing 25mM ammonium bicarbonate (pH 8.3), 10 mM D-proline, 0.25 mg porcine

D-amino acid oxidase(DAAO), 1000-2500 units bovine Catalase in a total volume of 1mL was incubated over night at 37°C. 100 µL sample from the reaction mixture in 25 mM ammonium bicarbonate buffer, adding 1mM NADPH and 6.5 µg HypS in a 1mL volume reaction. The enzyme activity catalyzed by HypS is measured by monitoring the reduction of NADPH.

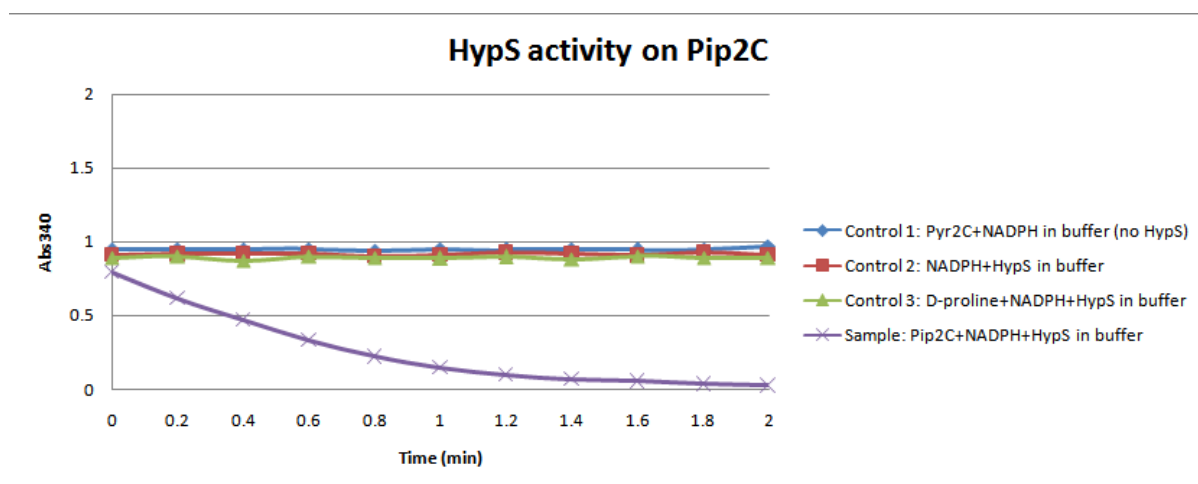


**Figure 14.** Relationship between absorbance and time following addition of 6.5 µg HypS to a 1 ml final volume reaction mixture containing 1 mM NADPH, 25 mM ammonium bicarbonate (pH 8.3) and 1 mM of  $\Delta^1$ -pyrroline-2-carboxylate (1:10 dilution of the D-proline, DAAO reaction mixture)

### ***S. meliloti* was tested on different carbon sources**

Wild type *S.meliloti* was examined for its ability to grow on various hydroxyproline isomers and L and D proline and lysine as carbon sources (Table 7). *S.meliloti* was unable to grow on *trans*-3-L-Hyp and D-lysine. It might attribute to the lack of enzyme to use *trans*-3-L-Hyp and the D-lysine uptake system.

**Table 7.** Growth of wild type *S. meliloti* on different carbon sources.

Carbon source (10mM)	Growth in M9 minimum media
<i>Trans</i> -4-L-Hyp	+++++
<i>Cis</i> -4-D-Hyp	+++++
<i>Trans</i> -4-D-Hyp	+++
<i>Trans</i> -3-L-Hyp	-

L-proline	+++++
D-proline	++
L-lysine	+++++
D-lysine	-

The “+”, “-” symbol showed in the table indicate the colony size

“+++++” – Large

“+++” – Medium

“++” – smaller than medium

“-” – Not grow

## Amino acid alignment and phylogenetic analysis

All the proteins belonging to the Ldh\_2 family are grouped into eight clades (Muramatsu et al., 2005a; Muramatsu et al., 2005b). However, they have diverse enzymatic functions other than MDH or LDH. There are two genes in *S. meliloti* annotated as malate/L-lactate dehydrogenase and belonging to the Ldh\_2 family, *smb20261* and *smc02035*. The HypS protein, encoded by *smb20261* falls into the DpkA clade. The DpkA clade contains homologs from *P. putida*, *P. syringae* and *P. aeruginosa*. DpkA was the first characterized  $\Delta^1$ -pyrroline-2-carboxylate/ $\Delta^1$ -piperidine-2-carboxylate reductase (Muramatsu et al., 2005b). HypS is also a  $\Delta^1$ -pyrroline-2-carboxylate reductase. The function of other two members in this clade is unknown (Muramatsu et al., 2005b).

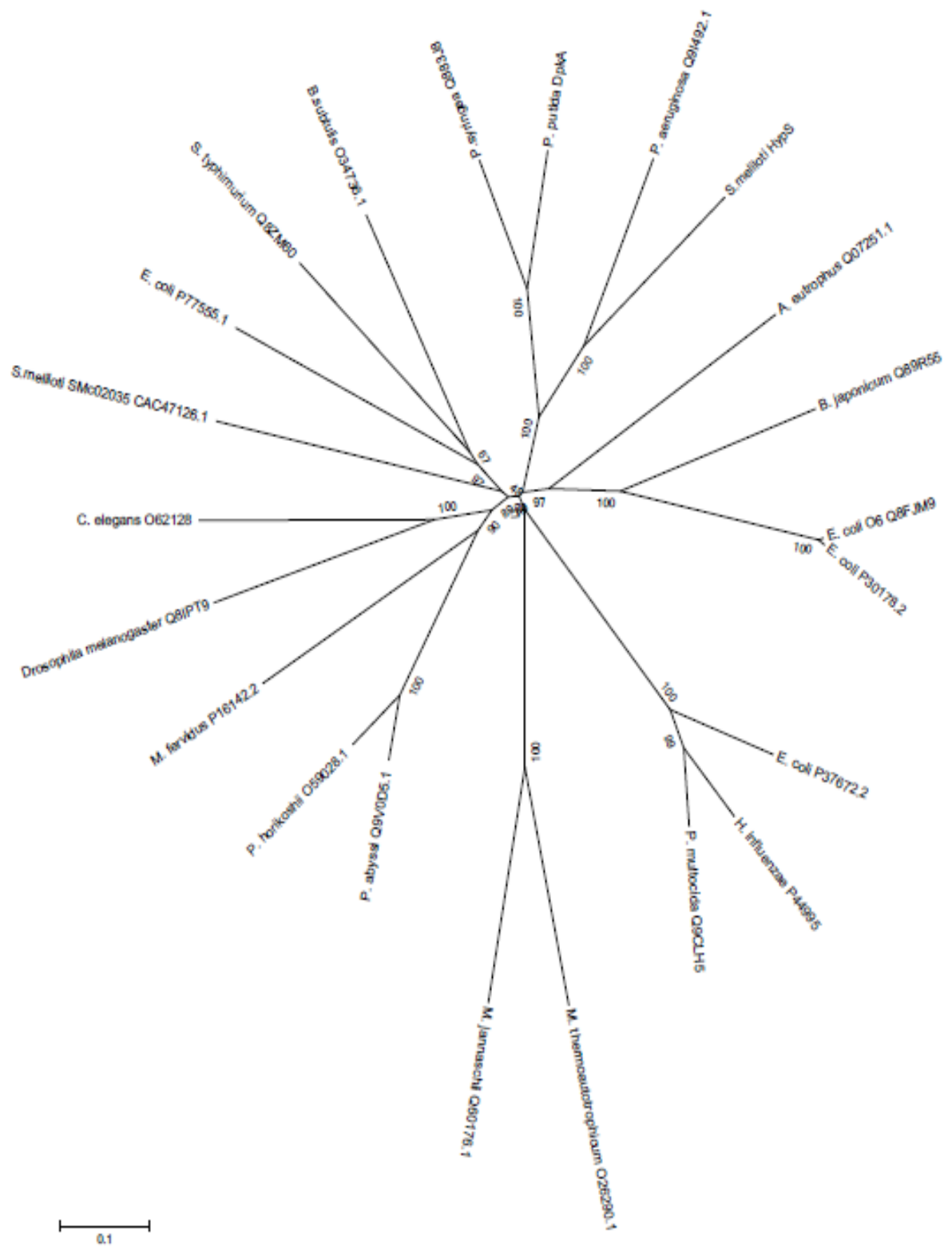


**Figure 15. Unrooted neighbour joining tree of Ldh\_2 family**

The scale bar represents 0.1 amino acid substitution per site. Bootstrap values (1000 bootstrap replicates) are indicated as percentage. The tree was made by MEGA 6 program (See Material and Method)

A multiple sequence alignment of DpkA clade from the above unrooted NJ tree was done by using MUSCLE. With the preference to its coenzyme NADPH, HypS has both conserved Arg<sup>310</sup> and Arg<sup>311</sup>, which is also conserved in DpkA and other two family members. That suggests they are showing the same coenzyme specificity.

Table 8 showed the sequence identity between those four proteins. The identity with HypS is lower than 60%. However, they have the same enzymatic functions.

```

P.syringae_Q883J8      MSASHADQPTQAVSYTQLIDLRLRIFVAHGTSPEVADVLAENCASAQRDGS SHGIFRIP
P._putida_DpkA        -MSAPSTSTVVRVPFTELQSLQAI FQRHGCS EAVARVLAHNCASAQRDGAHSHGVFRMP
P._aeruginosa_Q9I492.1 -----MIRMTLDEVRELAVRILRRHAFSEAHVQAVADTLVAGERDECASHGIWRLL
S.meliloti_HypS      -----MSETTTTLTTALQERVEAIFRKGGLNVVQAGALARVIVAGERDACKSHGIYRIE
                        :.  :.  * :  . .  . : *  . : : * * . * * : : * :
P.syringae_Q883J8      GYLSSLASGWVDGKAVPV-VEDVGA AFVVRVDACNGFAQPALAAARSLIDKALSAGVAIL
P._putida_DpkA        GYVSTLASGWVDGQATPQ-VSDVAAGYVRVDAAGGFAQPALAAARELLVAKARSAGIAVL
P._aeruginosa_Q9I492.1 GCIATLKAGKVSADAEPE-LHDIAPGLLRVDAHGGFSQCAFRLGLPHLLEKARSQGIAAM
S.meliloti_HypS      GALRTVKAGKVKPDAEPEIVAQEASAI VKNAGGGFANPAFELGLPVAERARKHGIAAL
                        * : : : * . * . * * : : . . . : * * * * : : * . * . * * : :
P.syringae_Q883J8      AIRGSHHFAALWPDVEPF AEQGLVALSMVNSMTCVVPHGARKPLFGTNP IAFGAPRAGGE
P._putida_DpkA        AIHNSHHFAALWPDVEPF AEGLVALSVVNSMTCVVPHGARKPLFGTNP IAFAPCAEHD
P._aeruginosa_Q9I492.1 AVNRCVHFSALWVEVEALTEAGLVALATTPSHAWVAPAGGRKPIFGTNP IAFGWPRPDGP
S.meliloti_HypS      AINDCTHFSALWPEAEALTEGGLAGLVMCP SYATVAPTGGNKPLLGTNP FAFGWPRAGKP
                        * : . * * : * * : * * : * * : * * : * * : * * : * * : * * .
P.syringae_Q883J8      PIVFDLATSIAIHGDVQIAAREGRLLPAGMGVDRDGLPTQEPRAILDGGALLPFGGHKGS
P._putida_DpkA        PIVFDMATSAMAHGDVQIAARAGQQLPEGMGVDADGQPTTDPKAILLEGGALLPFGGHKGS
P._aeruginosa_Q9I492.1 PFVDFFATS AVARGEIQLHERAGKPIPLGWGVDEQGEPTT DASAAL-RGAMLPFGGHKGS
S.meliloti_HypS      PYVDFFATSVAARGEIELHRRAGKPLPEGWAI DAQQGNPTT DPEAAL-AGAMLPFGGHKGS
                        * * * * : * * : * * : * * : * * : * * : * * : * * : * * : * * : * * :
P.syringae_Q883J8      ALSMMVELLAAGLTGGNFSFE-FDWSKHPGAQTPWTGQLLIVIDP----DKGAGQHFAQR
P._putida_DpkA        ALSMMVELLAAALTGGHFSWE-FDWSGHPGAQTPWTGQLIIVINP----GKAEGERFAQR
P._aeruginosa_Q9I492.1 ALAAMVELLAGPLIGDLTSAESLAYDEGS-RSSPYGGELLIAIDPRRMLGASAEHHLA-R
S.meliloti_HypS      AIGTMIELLAGIMIGDLTSPVLDYLGTT-TLAPFHGELIVAFSPQAF AAGRPGDPFA-R
                        * : . * * * * : * . * * : : . : * : * * : * * : * * : * * : * * :
P.syringae_Q883J8      SEELVRQLHGVGQERLPGI RRRYLERARSMAGIVIAQADLERLQELAGH-----
P._putida_DpkA        SRELVEHQAVGLTRMPGERRREREREVAEEGVAVTEQELQGLKELG-----
P._aeruginosa_Q9I492.1 AETLFEGIVEQG-ARLPSQRREARERSARDGVTIPEALHRELLALLE-----
S.meliloti_HypS      AELLFEAIVGQG-ARLPSQRREARAKSEAEGITLSAAEIEQLDRLLALGLDAVA
                        : * . : * * * * : * * : * * : * * : * * : * * : * * :

```

Figure 16. Partial multiple sequence alignment of DpkA clade.

**Table 8. Percent Identity Matrix - created by Clustal2.1**

Percent Identity Matrix	<i>P.syringae</i> _Q883J8	<i>P.putida</i> _DpkA	<i>P.aeruginosa</i> _Q91492.1	<i>S.meliloti</i> _HypS
<i>P.syringae</i> _Q883J8	100	68.62	42.25	<b>41.14</b>
<i>P. putida</i> _DpkA	68.62	100	44.38	<b>42.47</b>
<i>P. aeruginosa</i> _Q91492.1	42.25	44.38	100	<b>54.79</b>
<i>S. meliloti</i> _HypS	<b>41.14</b>	<b>42.47</b>	<b>54.79</b>	<b>100</b>

## Growth of $\Delta hypO$ , $D$ , $H$ , $S$ mutant

$\Delta hypO$ ,  $D$ ,  $H$ ,  $S$  mutant was grown in M9 minimum media supplemented *trans*-4-L-Hyp as carbon source. The generation times are summarized in Table 8. As the result showed, the  $\Delta hypS$  mutant grew as well as the wild type. The  $\Delta hypO$ , and  $\Delta hypH$  mutants grew more poorly, and this residual growth may have occurred as other enzymes with similar or the same activities may act in place of the mutant proteins. However, both the  $\Delta hypRE$  and  $\Delta hypD$  mutants were unable to grow in *trans*-4-L-Hyp, L-proline or sucrose.

$$G = \frac{(T2 - T1)}{\text{Log}_{10}(\text{OD}_{600\ 2} / \text{OD}_{600\ 1}) / \text{Log}_{10} 2}$$

**Table 9. Growth of  $\Delta hypO$ ,  $D$ ,  $H$ ,  $S$  mutant with *trans*-4-L-Hyp, L-proline or sucrose as the carbon source**

Strain	Generation Time			
	L-Hyp	L-Pro	Sucrose	D-Pro
RmP110(WT)	5.33±0.60	5.96±0.03	4.15±0.18	5.38±0.02
RmP2514( $\Delta hypS$ )	6.24±0.61	5.90±0.16	4.33±0.05	0
RmP2506( $\Delta hypO$ )	10.18±0.25	6.03±0.32	4.44±0.04	25.73±2.68
RmP2510( $\Delta hypD$ )	0	6.21±0.27	4.32±0.16	10.97±1.19
RmP2516( $\Delta hypH$ )	10.21±0.03	6.12±0.01	4.2±0.06	ND

All the strains were grown in 10mM L-Hyp, L-Pro, Sucrose or D-Pro as the carbon source. For L-Hyp, L-Pro, or Sucrose, the generation time was calculated between 0.1-0.2. For D-proline, it was calculated between 0.03-0.09.

ND - not determined

## HypH: KGSA dehydrogenase

### Growth of $\Delta araE \Delta hypH$ double mutant in liquid media

The growth of *S. meliloti* strains in M9 minimal media was measured by monitoring the OD<sub>600</sub> over 48 hours. The strains were grown in M9 with 15mM succinate as sole carbon source, 5mM L-hydroxyproline as sole carbon source or 5mM L-hydroxyproline as the sole

carbon and nitrogen source. While the wild type RmP110, and the  $\Delta araE$  mutant grew well in all three media, the  $\Delta hypH$  mutant grew slowly with L-hydroxyproline as carbon or nitrogen source while these strains grew well with succinate. The  $\Delta hypH \Delta araE$  double mutant failed to grow with L-hydroxyproline as carbon or nitrogen source consistent with the suggestion that the AraE  $\alpha$ -KGSA dehydrogenase isozyme was responsible for the growth of the  $\Delta hypH$  mutant on L-hydroxyproline.

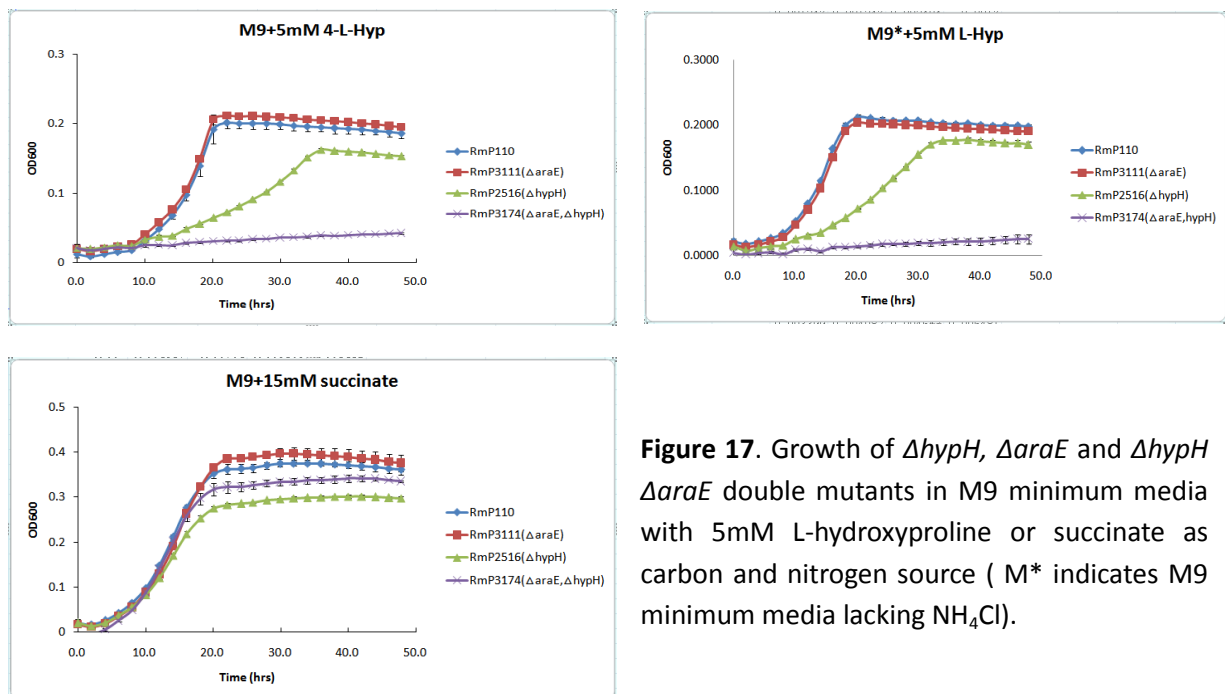


**Figure 17.** Growth of  $\Delta hypH$ ,  $\Delta araE$  and  $\Delta hypH \Delta araE$  double mutants in M9 minimum media with 5mM L-hydroxyproline or succinate as carbon and nitrogen source ( M\* indicates M9 minimum media lacking  $NH_4Cl$ ).

## Enzymatic characterization of HypH

$\alpha$ -KGSA was synthesized from D-glucarate by James Boudreau. In brief, D-glucarate is dehydrated to D-5-keto-4-deoxyglucarate(KDG) by D-glucarate dehydrogenase. Subsequently it converts to  $\alpha$ -KGSA by KDG dehydratase. The final concentration of  $\alpha$ -KGSA was calculated as 2.23 mM (See Material and Method and Figure 18). This was used to measure the enzyme

kinetics of HypH.

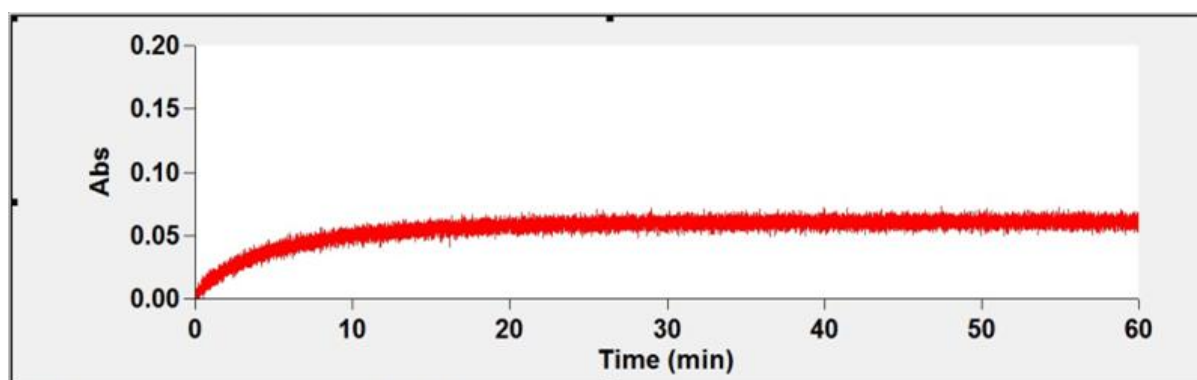


**Figure 18.** Relationship between absorbance and time following addition of 2.36  $\mu\text{g}$  HypH enzyme to reaction mixture containing 5  $\mu\text{L}$   $\alpha\text{-KGSA}$  stock solution and 0.5 mM  $\text{NADP}^+$  in 50mM Hepes buffer (pH 7.5) with 100 mM NaCl and 0.5 mM  $\text{MgCl}_2$

To determine the kinetic properties of the HypH catalyzed reaction, the initial rates of the enzyme were measured in triplicate assays at varying concentration of  $\alpha\text{-KGSA}$  (4.45, 11.1, 17.8, 22.3, 35.6, 44.5, 89.0, 133.6, 178.1  $\mu\text{M}$ ) and a constant concentration of 0.5 mM  $\text{NADP}^+$ . The reactions were run at room temperature by adding 2.36  $\mu\text{g}$  HypH enzyme in 50 mM Hepes buffer (pH 7.5) with 100 mM NaCl and 0.5 mM  $\text{MgCl}_2$  in a final volume of 1 mL. The product of the reaction was quantified by measuring the increase in absorbance at 340 nm. On the other hand, since this is a two components reaction, the reaction rate is also dependent on the cofactor  $\text{NADP}^+$  when the substrate  $\alpha\text{-KGSA}$  is saturated. To determine the kinetic constant of HypH for  $\text{NADP}^+$  in the presence of saturated  $\alpha\text{-KGSA}$  fixing at 178.1  $\mu\text{M}$ , the varying concentration of  $\text{NADP}^+$  at 10, 25, 50, 100, 300, 500  $\mu\text{M}$  or  $\text{NAD}^+$  at 0.2, 0.5, 1.0, 2.5, 4.0, 5.0, 8.0 mM were tested.

The velocity of the reaction was plotted against substrate concentration. The kinetic parameters were calculated by plotting the data to the Michaelis-Menten equation with

Origin 8.0. The data was obtained without inhibition by fitting the data to the following Michaelis-Menten equation (Fig 19). The kinetic parameters were summarized in Table 9.

The  $K_m$  value of  $NAD^+$  is 30-fold higher than  $NADP^+$ . As the consequence, the  $K_{cat}/K_m$  value of  $NADP^+$  is 210-fold higher than  $NAD^+$ . This result indicated that HypH is more  $NADP^+$  dependent enzyme.

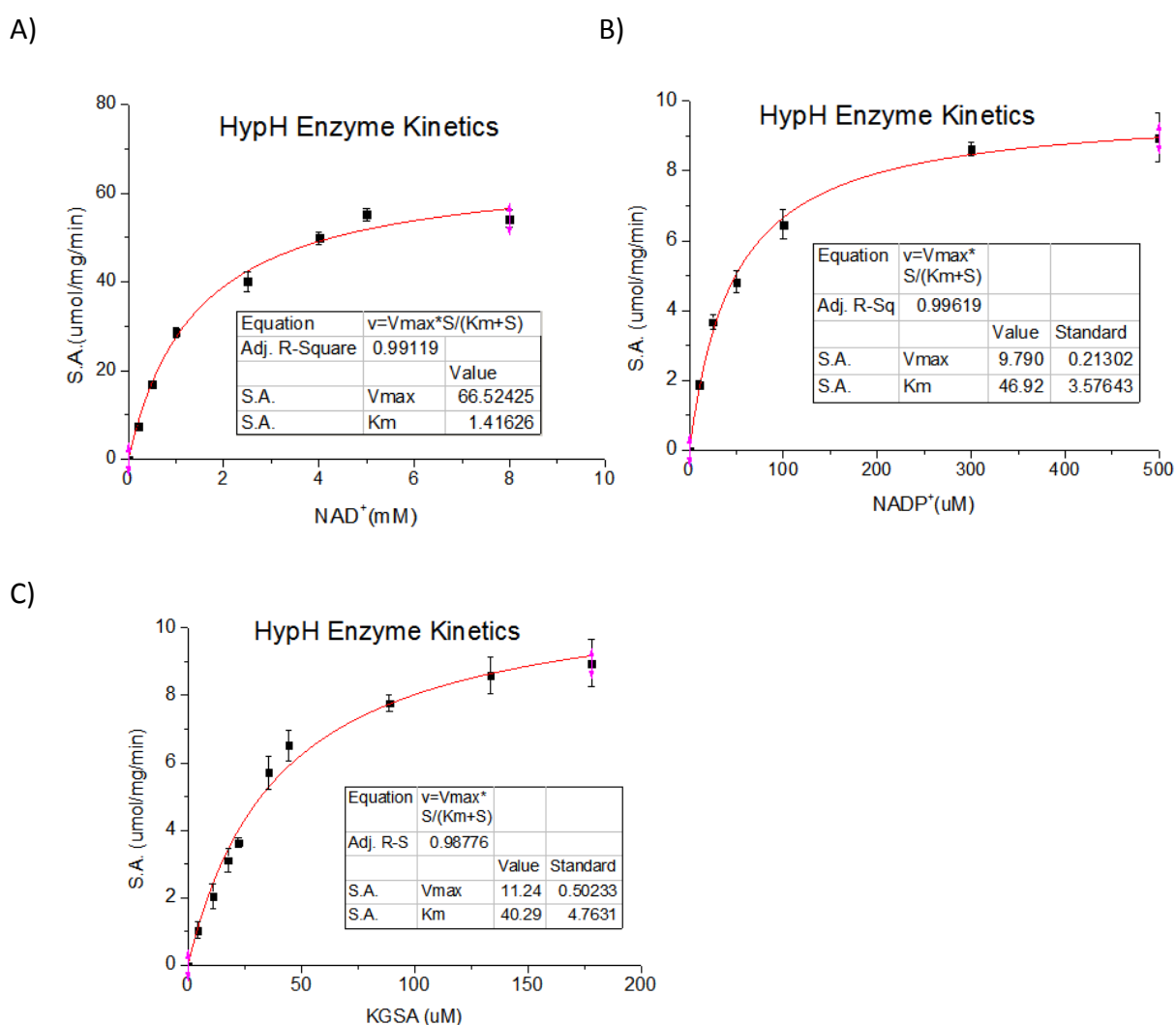


**Figure 19. HypH enzyme kinetics** A) The  $\alpha$ -KGSA concentration varied with a fixed concentration of  $NADP^+$  at 0.5mM. The data was plotted by using non-linear regression fitting by using equation 3. B) or C)The  $NADP^+$  or  $NAD^+$  concentration varied with a fixed concentration of  $\alpha$ -KGSA at 178.1  $\mu$ M. The data was plotted by using non-linear regression fitting by using M-M equation 3.

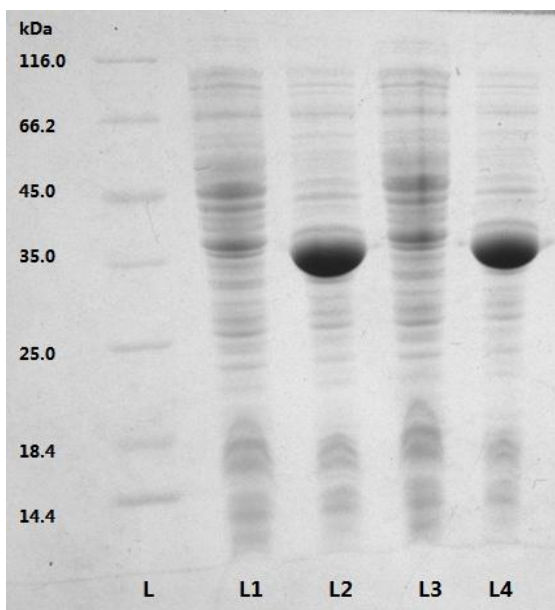
**Table 10.** The kinetic parameters of HypH.

	$\alpha$ -KGSA	NADP <sup>+</sup>	NAD <sup>+</sup>
Vmax ( $\mu\text{mol}/\text{min}/\text{mg}$ )	11.2	9.8	66.5
Km ( $\mu\text{M}$ )	40.3	46.9	1420
Kcat ( $\text{min}^{-1}$ )	628.6	550	3690.6
Kcat/Km ( $\mu\text{M}^{-1}\text{min}^{-1}$ )	15.6	11.7	0.0556

※Kcat=Vmax/[E]. Where MW of HypH is 505aa=505\*110=55.55kDa, so the concentration of the enzyme is  $1.18\text{mg}/\text{mL}=1.18/55.55*10^3=0.021\text{mM}$ . [E]=0.042 $\mu\text{M}$  Vmax=11.2 $\mu\text{mol}/\text{min}/\text{mg}$ =26.4mM/min. Therefore, Kcat=Vmax/[E]=628.6/min

### Purification of recombinant protein HypD

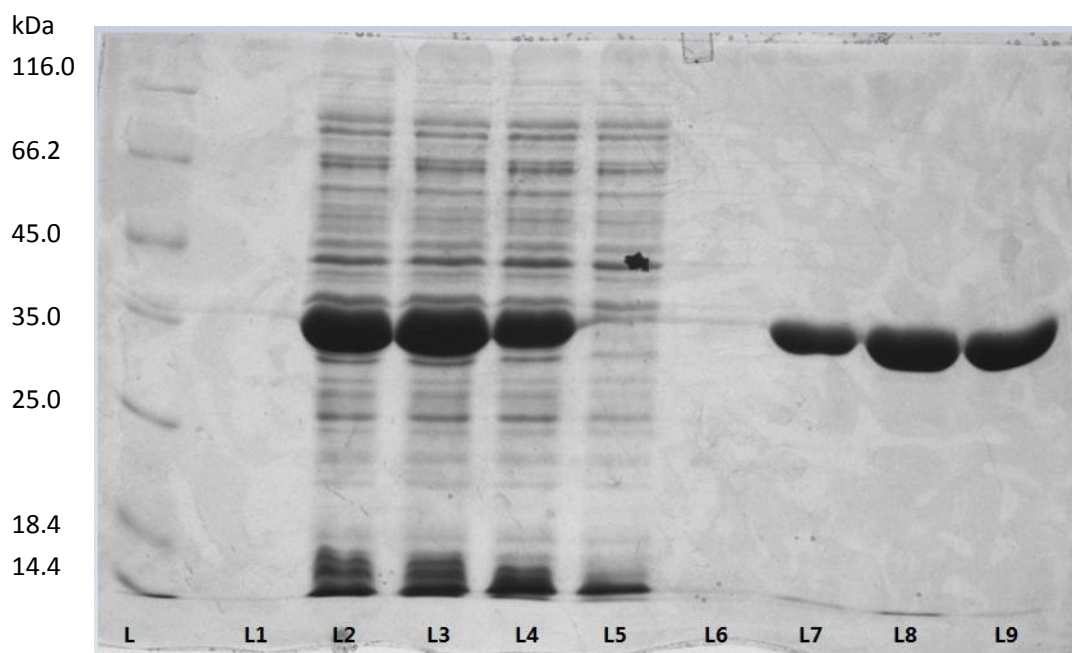
A small scale of *E. coli* culture (BL21/DE3 pLysS cells carrying the plasmid pTH2721) (5mL) were induced to investigate the percentage of over expressed protein in total protein. Induced cells were analyzed against the uninduced cells after they were normalized to same OD<sub>600</sub> and run on a 12% SDS-PAGE gel. HypD protein was prominent and appeared to be approximately 50% of total proteins in the cell.



L: Thermo Scientific Cat#PI-26610 Unstained protein ladder, L1: uninduced cell, L2: induced cell, L3: uninduced cell, L4: induced cell (L3 & L4 are duplicate)

**Figure.20** SDS-PAGE gel analysis of HypD over-expression in the whole cell extract (5mL culture)

We expressed a N-terminal His tag fusion construct of HypD protein in *E. coli*. The protein which was purified by a cobalt column showed high purity on the 12% SDS-PAGE gel. In Figure 20, the protein in the uninduced cell was missing in the Lane 1, as not much cell was in the sample. All the samples were prepared by 30  $\mu$ L cell culture mixed with 10  $\mu$ L 4X protein loading dye. The uninduced cells were not spun down to concentrate in 30  $\mu$ L, which made the concentration of the cell low in the loading sample (Fig 21 Lane 1).



Figure

#### SDS-PAGE gel analysis of HypD purification

L: Thermo Scientific Cat#PI-26610 Unstained protein ladder, L1: uninduced cell, L2: induced whole cell, L3: total lysate of French Press, L4: Supernatant after centrifugation at 24,000 RCF, L5: flow through, L6: Wash, L7, Pool fraction 1, L8: Pool fraction 2, L9: Pool fraction 3.

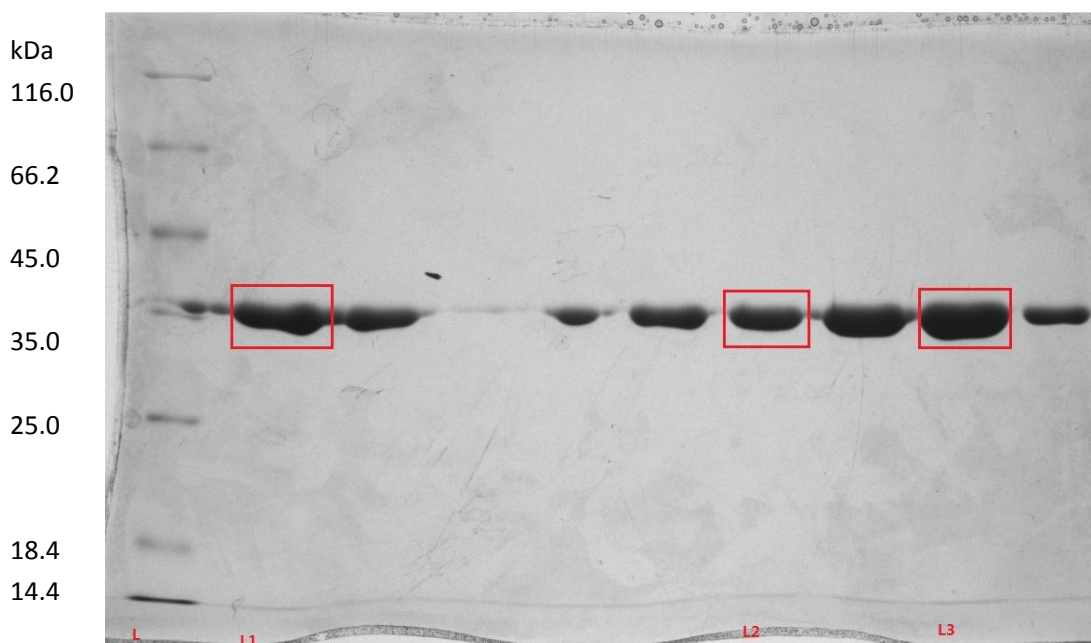


**Figure 22. SDS-PAGE gel analysis of the HypD purification**

L: Thermo Scientific Cat#PI-26610 Unstained Protein ladder, L1: Pool fraction 6, L2: Pool fraction 5, L3: Pool fraction 4

The concentration of protein was summarized in Table 11 and Appendix Table 13.

**Table 11. Protein concentration of each step**

Fractions	Fractions	OD595	Protein(mg/mL)	Protein (mg)
Whole cell	71.50	N/A	N/A	N/A
Total lysate	10.81	0.337(10X dil)	14.16	424.80
Supernatant	N/A	0.364(10X dil)	15.23	380.75
Fc1	F15-F20	0.696	<b>2.825</b>	16.95
Fc2 (5X dil)	F21-F27	0.244	<b>5.263</b>	36.84
Fc3 (5X dil)	F28-F33	0.262	<b>5.616</b>	33.69
Fc4	F34-F40	0.640	<b>2.606</b>	18.24
Fc5	F41-F50	0.509	<b>2.092</b>	20.92
Fc6	F51-F60	0.387	<b>1.613</b>	16.13
<b>Final protein</b>	<b>6.28mg/mL</b>	<b>40.19mg (32 tubes)</b>		

### HypD enzymatic assay : Couple assay with HypH

HypD protein is a deaminase which can convert  $\Delta^1$ -pyrroline-4-hydroxy-2-carboxylate (HPC) to  $\alpha$ -KGSA. HPC was synthesized from *cis*-4-D-Hyp by using HypO protein purified by

Guia (Material and Method). HypD activity was couple assayed with HypH spectrophotometrically. The activity was measured by the formation of NADPH, which was the only molecule in the mixture absorbs light at 340 nm. The 1 mL reaction mixture consisted of 50 mM Tris-HCl buffer (pH 8.0), 100  $\mu$ L from the HPC product mixture (PMS is not removed), 0.5 mM NADP<sup>+</sup> and 10.34  $\mu$ g HypH. The absorbance change was measured over 60 minutes after adding 12.56  $\mu$ g HypD.

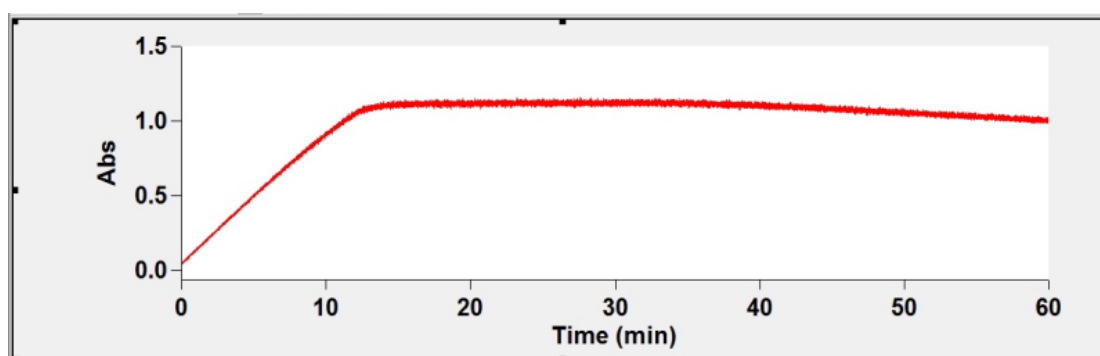


**Figure 23.** Relationship between absorbance and time following addition of 12.56  $\mu$ g HypD enzyme to reaction mixture containing 100  $\mu$ L HPC solution, 0.5 mM NADP<sup>+</sup> and 10.34  $\mu$ g HypH in 50 mM Tris-HCl buffer (pH 8.0).

Figure 23 showed that NADPH accumulated after adding the HypD protein. That indicated HypD converted HPC to  $\alpha$ -KGSA, which subsequently produced  $\alpha$ -KG by HypH. In addition, when the reaction reached its equilibrium, the absorbance slightly decreased. The reason accounted for this is the presence of phenazine methosulfate (PMS), which not only will degrade in light, but will also promote the conversion from NADPH to NADP<sup>+</sup> (Muirhead and Hothersall, 1995).

To investigate if HypO, HypD, HypH react on *cis*-4-D-Hyp continuously, a 1 mL reaction mixture containing 50 mM Tris-HCl buffer (pH 8.0), 2 mM MgCl<sub>2</sub>, 50 mM *cis*-4-D-Hyp, 0.05 mM PMS, 0.5 mM NADP<sup>+</sup> and 38  $\mu$ g HypO, 12.56  $\mu$ g HypD and 10.34  $\mu$ g HypH. The absorbance was measure over 120 minutes.

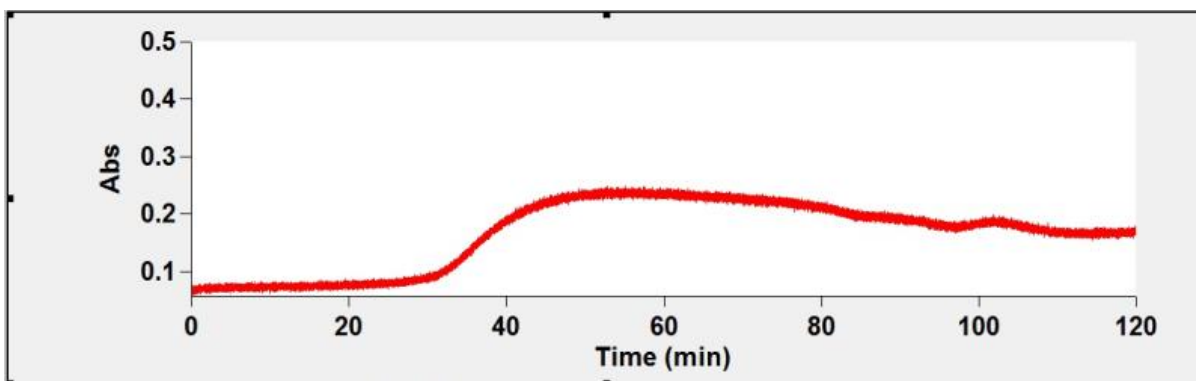


**Figure 24.** Relationship between absorbance and time with HypO, HypD, HypH on *cis*-4-D-Hyp. Reaction mixture containing 50 mM Tris-HCl buffer (pH 8.0), 2 mM MgCl<sub>2</sub>, 50 mM *cis*-4-D-Hyp, 0.05 mM PMS, 0.05 mM NADP<sup>+</sup> and 38 μg HypO, 12.56 μg HypD and 10.34 μg HypH.

The figure 24 showed that HPC slowly started to obtain from *cis*-4-D-Hyp and converted to α-KG by HypD and HypH. The rate became faster after 30 minutes, as it took time to synthesize HPC by HypO in the early period of time. After 60 minute the absorbance started to slightly decrease due to the presence of PMS. However, there was no activity observed when PMS was absence in the reaction (data not shown).

### **HypO couple assay with HypS on *cis*-4-D-Hyp**

HPC mixture was synthesized from *cis*-4-D-Hyp (Material and Method). It contained certain amount of *cis*-4-D-Hyp left, HypO and 0.005 mM PMS (after 24 hours incubation in the dark). 1 mL reaction consisted of 100 μL HPC reaction mixture, 0.5 mM NADPH in 50mM Tris-HCl (pH 8.0) with addition of 9.75 μg HypS. Absorbance change was observed over 30 minutes. Even though PMS interfered the reaction, but the concentration of PMS was lower than 0.005 mM after incubation in 30°C overnight. While a fresh 0.005 mM PMS significantly interacted with NADPH (Figure 25 C and D). That explained the decrease of absorbance of figure 25A and B was not as significant as figure 25C and D. However, it

cannot tell if HypS had activity on HPC unless PMS was removed.

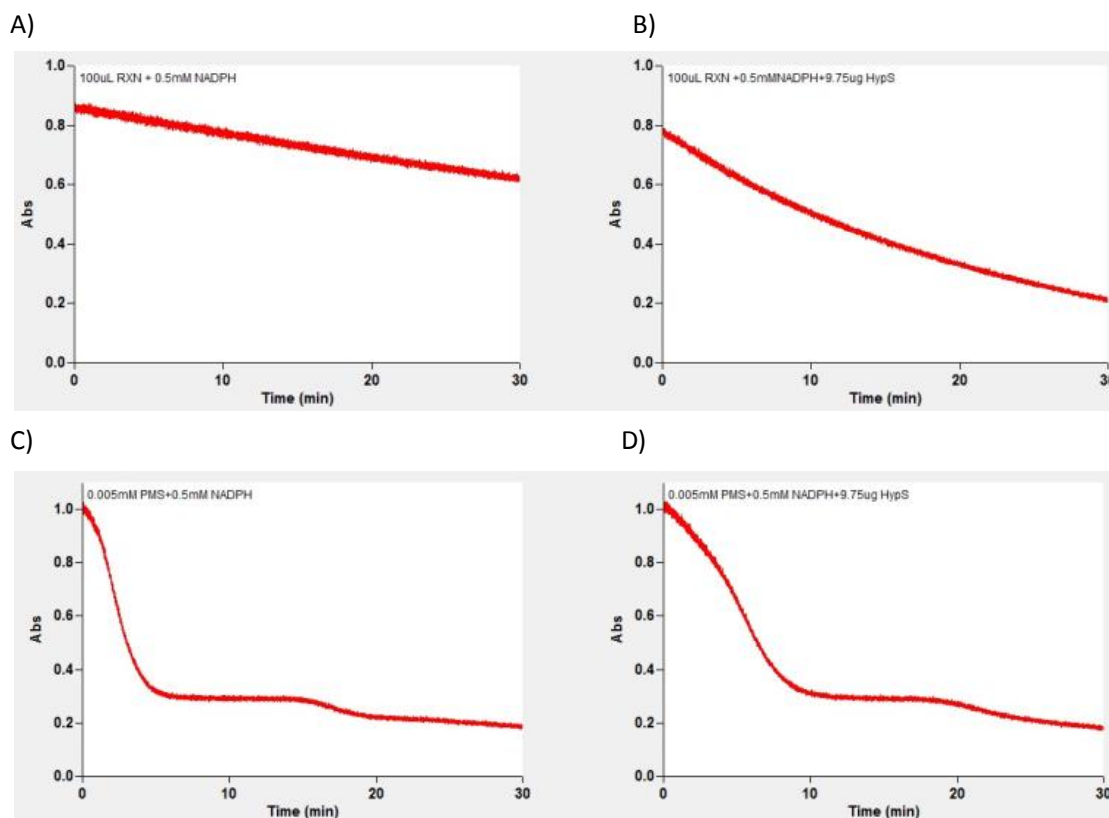


**Figure 25.** Relationship between absorbance and time on HPC catalyzed by HypS. A) 100  $\mu$ L HPC reaction mixture (containing 0.005 mM PMS, HypO and certain amount of *cis*-4-D-Hyp), 0.5 mM NADPH in 50 mM Tris-HCl (pH 8.0). B) 100  $\mu$ L HPC reaction mixture (containing 0.005 mM PMS, HypO and certain amount of *cis*-4-D-Hyp), 0.5 mM NADPH in 50 mM Tris-HCl (pH 8.0) with addition of 9.75  $\mu$ g HypS. C) 0.005 mM fresh PMS, 0.5 mM NADPH in 50 mM Tris-HCl (pH 8.0). D) 0.005 mM fresh PMS, 0.5 mM NADPH in 50 mM Tris-HCl (pH 8.0) with addition of 9.75  $\mu$ g HypS

## CONCLUSION AND DISCUSSION

### HypS is a $\Delta^1$ -pyrroline-2-carboxylate reductase

The data presented in this thesis suggests that HypS is a  $\Delta^1$ -pyrroline-2-carboxylate reductase, which reduces  $\Delta^1$ -pyrroline-2-carboxylate to L-proline. Kinetic analyses showed HypS prefers NADPH to NADH as an enzyme cofactor. Interestingly,  $\Delta^1$ -pyrroline-2-carboxylate will spontaneously open its ring to become a chain compound  $\alpha$ -keto- $\delta$ -aminovalerate (Figure 26). Likewise, the oxidation product HPC from *cis*-4-D-Hyp can also open to a chain compound 2-oxo-4-hydroxy-5-aminovalerate. Since the similar structure of Pyr2C and HPC, it will naturally imply HypS might have some activity on HPC, or HypD might have some activity on Pyr2C.

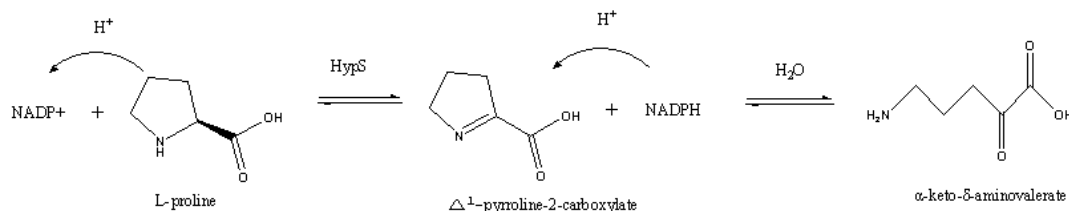


**Figure 26.** Schematic diagram showing the reaction between L-proline and Pyr2C.

### Physiological function of HypS

*hypS* is one of 14 genes located in the hydroxyproline locus on pSymb and one of the goals of this study was to investigate the physiological function of HypS. Transcription of *hypS* is negatively regulated by HypR and it is significantly induced when hydroxyproline is present in the media (White et al., 2012a). Interestingly as a *hypS*<sup>-</sup> mutant grew well on L-hydroxyproline as the sole carbon source, HypS does not appear to play a direct role in

L-hydroxyproline catabolism. Wild type *S. meliloti* was found to grow on D-proline as the sole carbon source, whereas the *hypS*<sup>-</sup> mutant strain did not grow on D-proline. Thus *hypS* was required for *S. meliloti* to utilize D-proline and as discussed below, additional evidence strongly suggests that the D-proline catabolic pathway involves its conversion to L-proline. *S. meliloti* carries several proteins annotated as D-amino acid oxidases (Smb20267) that could presumably oxidize D-proline to Pyr2C (Pollegioni et al., 1997). Thus upon transport into the cells, we envisage D-amino acid oxidase as converting D-proline to Pyr2C and the Pyr2C is subsequently converted to L-proline by HypS. As the grow curve showed (Figure 10), there was a lag exhibited on D-proline and the cells were not using this carbon source as efficiently as other carbon sources, such as L-hydroxyproline or L-proline. Furthermore, another question might be addressed how D-proline transports into the cell. The uptake system of D-proline probably shares the transport systems of hydroxyproline or L-proline. However, the role of *hypS* in hydroxyproline catabolism is still unknown and under investigated in the future.

### **Comparison to other Pyr2C reductase.**

In microbial system, DpkA enzyme in *P. putida* was the first enzyme to be characterized as  $\Delta^1$ -piperideien-2-carboxylate/ $\Delta^1$ -pyrroline-2-carboxylate reductase (Muramatsu et al., 2005b). Both HypS and DpkA proteins belong to the Ldh\_2 family. HypS shows high enzymatic function similarity with DpkA, such as substrate specificity, cofactor, optimum pH, enzymatic kinetics. Nevertheless as the data showed, although HypS can reduce  $\Delta^1$ - piperideien-2-carboxylate to L-pipercolate (Figure 14). *S. meliloti* is unable to

grow on D-lysine as the carbon source. The reason is accounted for the *S. meliloti* is unable to transport D-lysine to the cell.

### **Are some *hyp* genes present in other organisms?**

Since there is the *hyp* operon in *S. meliloti* that catabolize hydroxyproline and provide nutrition to the bacteria, it is interesting to see if some *hyp* genes are present in other organisms. Similar proteins were defined from STRING database (Franceschini et al., 2013) and the gene map was made from BIOCYC (Caspi et al., 2014). *Rhizobium leguminosarum* *bv. viciae* has the symbiotic relationship with several legume plants, such as pea and vetch (Karunakaran et al., 2009). There is part of the hydroxyproline genes present in *R. leguminosarum* (Figure 27). Four genes *pRL\_120528*, *120529*, *120530*, *120535* in the known pathway and the ABC-transport system genes *pRL\_120532*, *120533*, *120534* were present and might be up-regulated by *pRL\_120527* gene. *Burkholderia ambifaria*, a member of *Burkholderia cepacia* complex of betaproteobacteria, had been found in various environments, such as water, soil, rhizosphere of plants, human and many animal species and hospital environments (Coenye and Vandamme, 2003). The predicted hydroxyproline gene cluster in this organism also includes the genes for the transport system and the known pathway, and it is regulated by *BamMC406\_3224*. *B. petrii* was a genus *bordetella* isolated from human. It is interesting that hydroxyproline catabolism cluster also present in this bacterium. Furthermore, HypS-like protein is also located between the HypO-like and HypRE-like proteins. In addition, *hyp* genes are also found in *P. putida*, *P. aeruginosa* and marine bacteria *C. psychrerythraea* (Watanabe et al., 2014). It is naturally speculated that

hydroxyproline cluster is not only found in soil bacteria that fix nitrogen, but it is also present in other organisms.

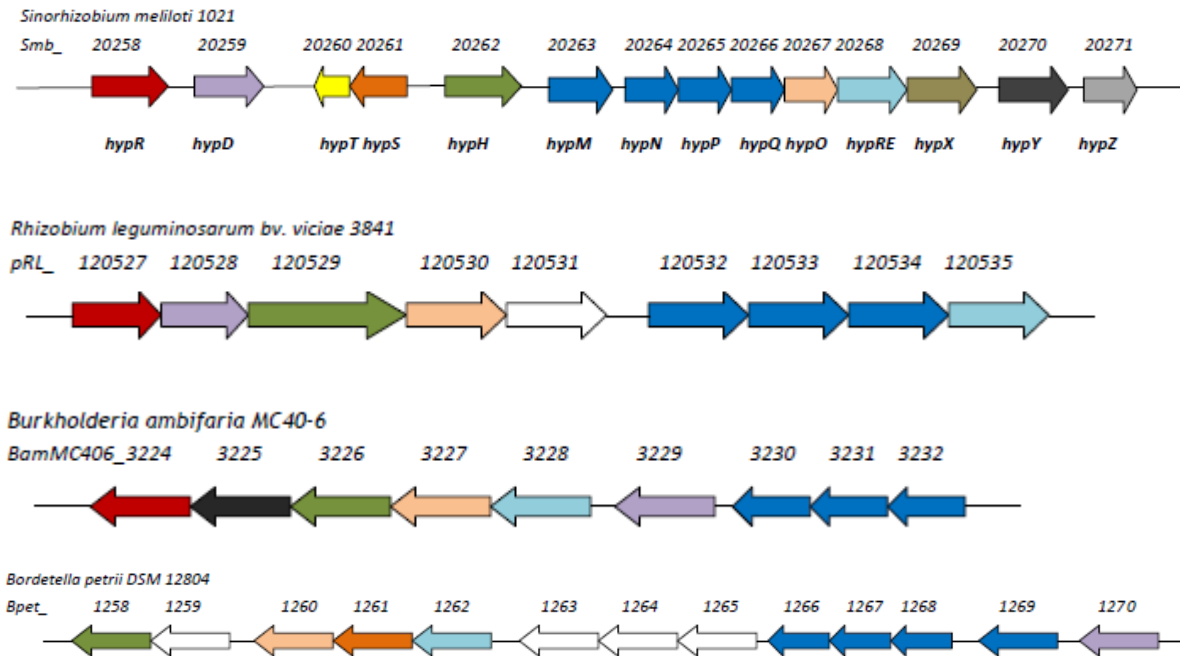


**Figure 27.** Schematic of gene clusters related to 4-hydroxyproline catabolism of bacteria. Same color predicts same enzymatic functions. White color predicts the gene is not involved in hydroxyproline catabolism.

## APPENDIX

**Table 12. Strains and plasmids used in this study.**

Strains or plasmids	Description	Antibiotics Resistance	Reference
<b><i>S. meliloti</i></b>			
RmP110	Rm1021 with wild type <i>pstC</i>	Sm <sup>r</sup>	Yuan <i>et al.</i> , 2006
Rm1021	SU47 str-21 (wild type)	Sm <sup>r</sup>	Yuan <i>et al.</i> , 2006
RmP2514	RmP110 $\Delta$ <i>smb20261::FRT</i> ; non-polar deletion of <i>smb20261</i> . FLP introduced into RmP2513 (then strain cured of the FLP vector (pTH2505))	Sm <sup>r</sup>	White <i>et al.</i> , 2012
RmP3144	RmP110 <i>proC::Tn5-B20</i> transposon inserted within the <i>proC</i> gene	Sm <sup>r</sup> , Nm <sup>r</sup>	diCenzo, unpublished data
RmP2707	RmP110 $\Delta$ B161, 60kb deletion on pSymB that includes <i>smb20003</i> . This deletion was made using FRT sites and FLP recombinase.	Sm <sup>r</sup> , Nm <sup>r</sup> , Gm <sup>r</sup> , Tet <sup>r</sup>	Mulunovic <i>et al.</i> , 2014
RmP2506	RmP110 $\Delta$ <i>smb20267::FRT</i> ; non-polar deletion of <i>smb20267</i> . FLP introduced into RmP2505 (then strain cured of the FLP vector (pTH2505))	Sm <sup>r</sup>	White <i>et al.</i> , 2012
RmP2508	RmP110 $\Delta$ <i>smb20268::FRT</i> ; non-polar deletion of <i>smb20268</i> . FLP introduced into RmP2507 (then strain cured of the FLP vector (pTH2505))	Sm <sup>r</sup>	White <i>et al.</i> , 2012
RmP2510	RmP110 $\Delta$ <i>smb20269::FRT</i> ; non-polar deletion of <i>smb20259</i> . FLP introduced into RmP2509 (then strain cured of the FLP vector (pTH2505))	Sm <sup>r</sup>	White <i>et al.</i> , 2012
RmP2718	RmP110 $\Delta$ B141 ~300kb deletion incl. <i>hyp</i> locus	Sm <sup>r</sup>	Mulunovic <i>et al.</i> , 2014
RmP3152	$\Phi$ RmP3144(Nm <sup>r</sup> ) $\rightarrow$ RmP2514, <i>proC</i> , $\Delta$ <i>hypS</i>	Nm <sup>r</sup> , Sm <sup>r</sup>	This study
RmP3153	$\Phi$ RmP2707(Gm <sup>r</sup> ) $\rightarrow$ RmP3152, <i>proC</i> , $\Delta$ <i>hypS</i> , $\Delta$ <i>smb20003</i>	Gm <sup>r</sup> , Nm <sup>r</sup> , Sm <sup>r</sup>	This study
RmP3154	$\Phi$ RmP2707(Gm <sup>r</sup> ) $\rightarrow$ RmP2514, $\Delta$ <i>smb20003</i> , $\Delta$ <i>hypS</i>	Gm <sup>r</sup> , Nm <sup>r</sup> , Sm <sup>r</sup>	This study
RmP3155	$\Phi$ RmP2707(Gm <sup>r</sup> ) $\rightarrow$ RmP3144, $\Delta$ <i>smb20003</i> , <i>proC</i>	Gm <sup>r</sup> , Nm <sup>r</sup> , Sm <sup>r</sup>	This study
RmFL5502	RmP110 <i>putA::gfp+/lacZ</i> pFL5502 (268,250 to 268,699 nucleotides)	Sm <sup>r</sup> , Gm <sup>r</sup>	Cowie <i>et al.</i> , 2006
RmP1114	RmP110 $\Delta$ <i>hypMNPQ</i> ( $\Delta$ <i>smb20263</i> - <i>smb20266</i> ) via excision of pTH2131 to generate in-frame deletion	Sm <sup>r</sup>	MacLean <i>et al.</i> , 2009
RmP3272	RmP2514(pTH2685), integration of pTH2685 into pSymB by single cross-over	Sm <sup>r</sup> , Gm <sup>r</sup>	This study
RmP239	Rm1021 with <i>hypS::gusA</i> (pTH1360 integrant)	Sm <sup>r</sup> , Nm <sup>r</sup>	White <i>et al.</i> , 2012
RmP1886	RmP110 with <i>hypM::gusA</i>	Sm <sup>r</sup> , Gm <sup>r</sup>	MacLean <i>et al.</i> , 2009
RmFL2315	RmP110 with <i>hypR::gusA</i>	Sm <sup>r</sup> , Gm <sup>r</sup>	Cowie <i>et al.</i> , 2006

RmFL866	RmP110 with <i>hypS::lacZ</i> , <i>hypH::gusA</i>	Sm <sup>r</sup> , Gm <sup>r</sup>	Cowie <i>et al.</i> , 2006
RmP2551	RmP110 with <i>hypO::lacZ</i>	Sm <sup>r</sup> , Gm <sup>r</sup>	White <i>et al.</i> , 2012
RmP2516	RmP110 $\Delta$ <i>smb20262::FRT</i> ; non-polar deletion of <i>smb20262</i> FLP introduced into RmP2515 (then strain cured of the FLP vector (pTH2505))	Sm <sup>r</sup>	White, Unpublished
RmP3111	Rm2011, <i>araE::Tn5</i>	Sm <sup>r</sup> , Nm <sup>r</sup>	Oresnik
RmP3174	$\Phi$ RmP3111(Nm <sup>r</sup> ) $\rightarrow$ RmP2516, <i>araE</i> , $\Delta$ <i>hypH</i>	Sm <sup>r</sup> , Nm <sup>r</sup>	This Study
<b><i>E. coli</i></b>			
MT616	MT607 (pRK600)	Cm <sup>r</sup>	Finan <i>et al.</i> , 1986
M1859	DH5 $\alpha$ ( <i>Smb20259</i> cloned into pET28a for over-expression with an N-terminal His6 tag.)	Kan <sup>r</sup>	White, unpublished data
<b>Plasmid</b>			
pTH2685	<i>smb20261</i> + flanking DNA in pUCP30T for replacing <i>Smb20261</i> with FRT-kan-FRT	Gm <sup>r</sup>	White, unpublished data
pTH1360	pVO155 derivative with <i>gusA</i> from pFUS1	Nm <sup>r</sup> , Amp <sup>r</sup>	Zaheer <i>et al.</i> , 2009

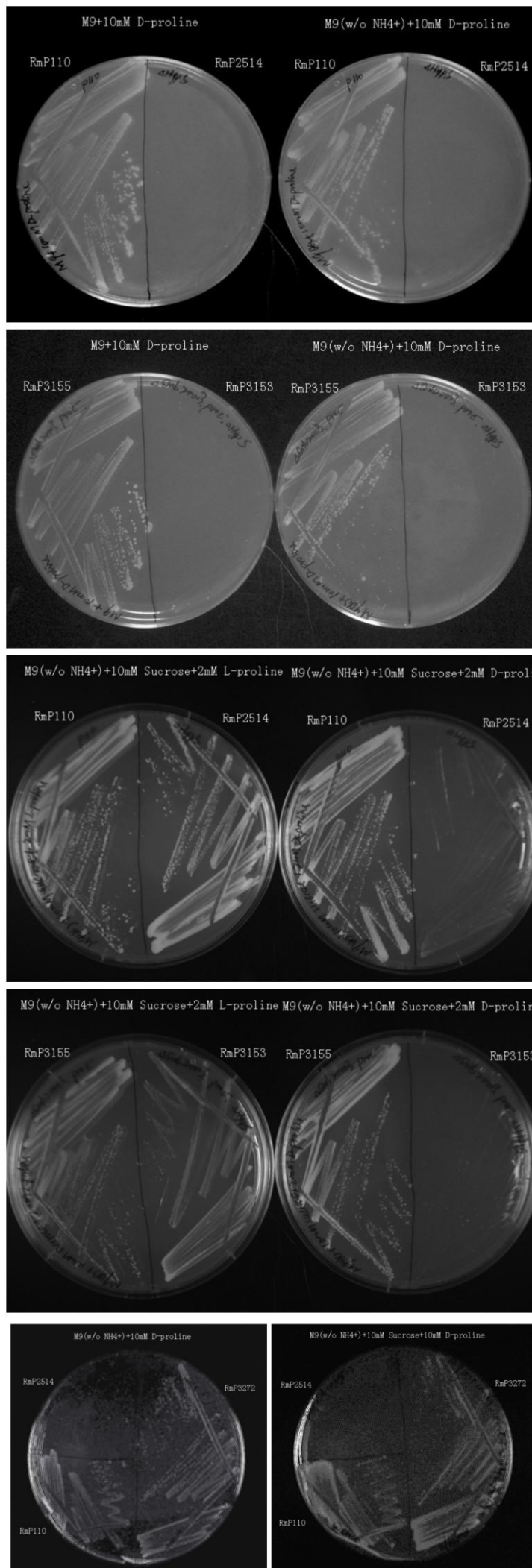


**Figure 28.** Growth of hypS mutant, L-proline auxotroph, and its derivative on minimum agar plate.

**Table.13 Protein concentration of each eluted fractions**

Fractions	OD595	Protein(mg/mL)	Fractions	OD595	Protein(mg/mL)	Fractions	OD595	Protein(mg/mL)
F1	0.000	<b>0.096</b>	F21	0.900	<b>3.625</b>	F41	0.512	<b>2.104</b>
F2	-0.002	<b>0.088</b>	F22	0.874	<b>3.523</b>	F42	0.492	<b>2.025</b>
F3	0.000	<b>0.096</b>	F23	0.909	<b>3.660</b>	F43	0.495	<b>2.037</b>
F4	-0.013	<b>0.045</b>	F24	0.949	<b>3.817</b>	F44	0.431	<b>1.786</b>
F5	-0.006	<b>0.072</b>	F25	0.898	<b>3.617</b>	F45	0.446	<b>1.845</b>
F6	0.002	<b>0.104</b>	F26	0.942	<b>3.790</b>	F46	0.410	<b>1.704</b>
F7	0.001	<b>0.100</b>	F27	0.875	<b>3.527</b>	F47	0.407	<b>1.692</b>
F8	0.006	<b>0.119</b>	F28	0.871	<b>3.511</b>	F48	0.379	<b>1.582</b>
F9	0.011	<b>0.139</b>	F29	0.933	<b>3.755</b>	F49	0.396	<b>1.649</b>
F10	0.016	<b>0.159</b>	F30	0.918	<b>3.696</b>	F50	0.349	<b>1.464</b>
F11	0.030	<b>0.213</b>	F31	0.922	<b>3.711</b>	F51	0.344	<b>1.445</b>
F12	0.023	<b>0.186</b>	F32	0.855	<b>3.449</b>	F52	0.379	<b>1.582</b>
F13	0.039	<b>0.249</b>	F33	0.834	<b>3.366</b>	F53	0.338	<b>1.421</b>
F14	0.058	<b>0.323</b>	F34	0.740	<b>2.998</b>	F54	0.352	<b>1.476</b>
F15	0.117	<b>0.555</b>	F35	0.726	<b>2.943</b>	F55	0.335	<b>1.409</b>
F16	0.356	<b>1.492</b>	F36	0.674	<b>2.739</b>	F56	0.317	<b>1.339</b>
F17	0.562	<b>2.300</b>	F37	0.654	<b>2.660</b>	F57	0.315	<b>1.331</b>
F18	0.715	<b>2.900</b>	F38	0.650	<b>2.645</b>	F58	0.309	<b>1.308</b>
F19	0.764	<b>3.092</b>	F39	0.631	<b>2.570</b>	F59	0.296	<b>1.257</b>
F20	0.762	<b>3.084</b>	F40	0.505	<b>2.076</b>	F60	0.276	<b>1.178</b>

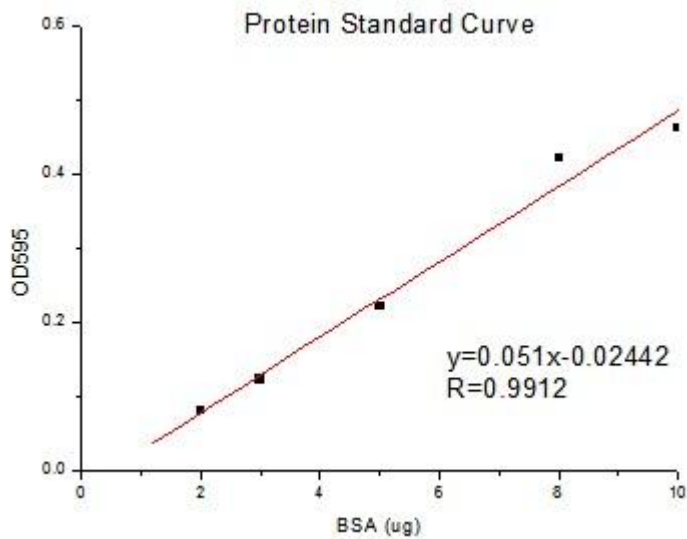


**Figure.29 Protein Standard curve (BSA) by using Bio-Rad protein assay**

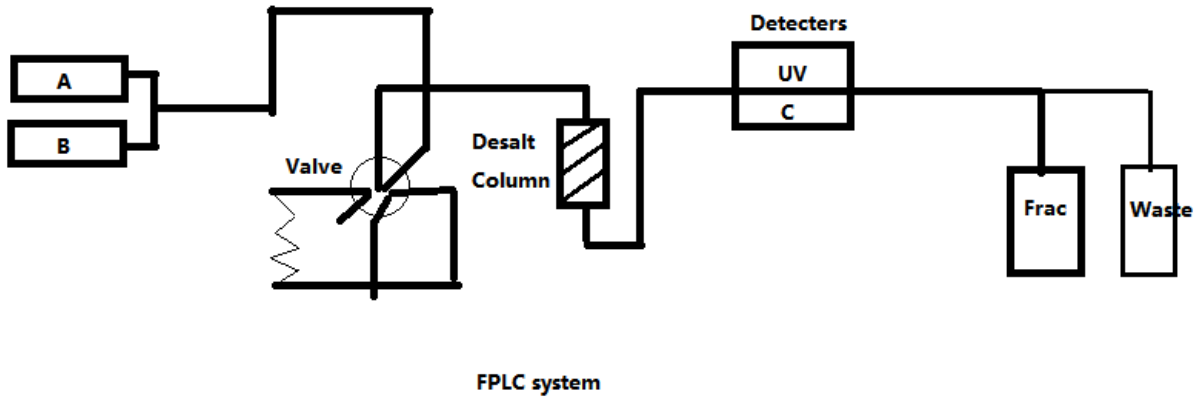


**Figure 30. Schematic of FPLC system connection.** Proteins were detected by UV light at OD<sub>280</sub>. The ionic conductivity was detected as well. Fractions were collected when the target protein eluted and stop collection until all the proteins have been eluted. Let the storage buffer flush the system until the conductivity goes smoothly prior to load the second sample. The flow rate of the running buffer is set to 5mL/min.

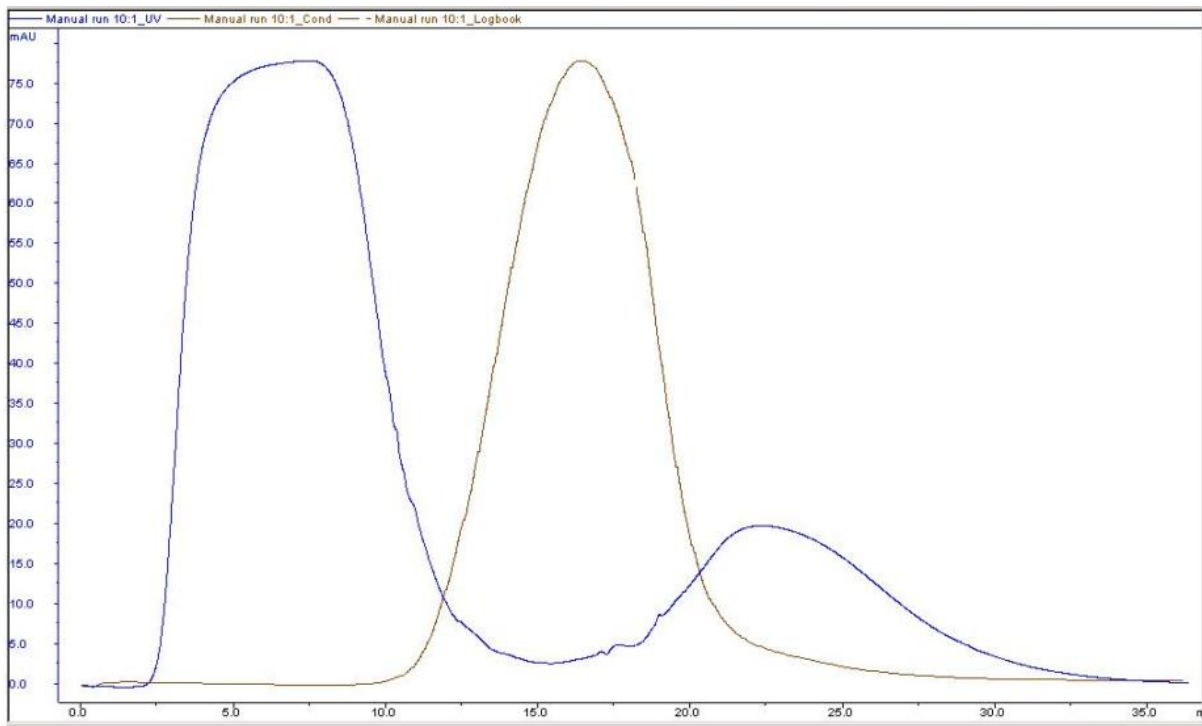


**Figure 31. Chromatogram of fraction 2&3.**

A chromatogram is absorbance change at 280nm (Blue)/percentage of conductivity (Brown) versus volume of running buffer. Protein started to elute at about 0.5 minute to 2.5 minute. (2.5 mL - 12.5 mL running buffer).

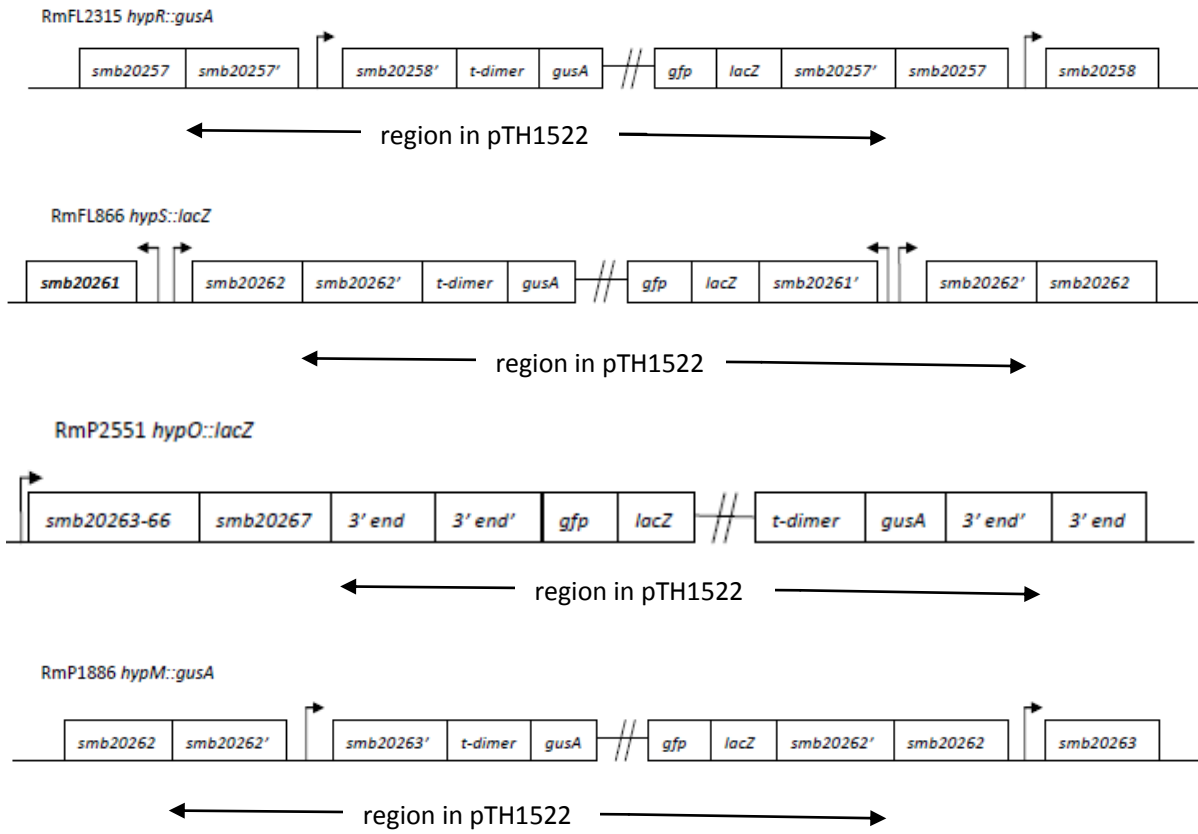


**Figure 32.** Schematic of gene fusions.

## REFERENCES

- Adams, E., and Frank, L. (1980). Metabolism of Proline and the Hydroxyprolines. *Annual Review of Biochemistry* *49*, 1005-1061.
- Bater, A.J., Venables, W.A., and Thomas, S. (1977). Allohydroxy-D-proline dehydrogenase. An inducible membrane-bound enzyme in *Pseudomonas aeruginosa* PA01. *Arch Microbiol* *112*, 287-289.
- Caspi, R., Altman, T., Billington, R., Dreher, K., Foerster, H., Fulcher, C.A., Holland, T.A., Keseler, I.M., Kothari, A., Kubo, A., *et al.* (2014). The MetaCyc database of metabolic pathways and enzymes and the BioCyc collection of Pathway/Genome Databases. *Nucleic Acids Res* *42*, 12.
- Coenye, T., and Vandamme, P. (2003). Diversity and significance of Burkholderia species occupying diverse ecological niches. *Environ Microbiol* *5*, 719-729.
- Cooper, J.E. (2007). Early interactions between legumes and rhizobia: disclosing complexity in a molecular dialogue. *J Appl Microbiol* *103*, 1355-1365.
- Cowie, A., Cheng, J., Sibley, C.D., Fong, Y., Zaheer, R., Patten, C.L., Morton, R.M., Golding, G.B., and Finan, T.M. (2006a). An Integrated Approach to Functional Genomics: Construction of a Novel Reporter Gene Fusion Library for *Sinorhizobium meliloti*. *Applied and Environmental Microbiology* *72*, 7156-7167.
- Cowie, A., Cheng, J., Sibley, C.D., Fong, Y., Zaheer, R., Patten, C.L., Morton, R.M., Golding, G.B., and Finan, T.M. (2006b). An integrated approach to functional genomics: construction of a novel reporter gene fusion library for *Sinorhizobium meliloti*. *Appl Environ Microbiol* *72*, 7156-7167.
- Ferrieres, L., Francez-Charlot, A., Gouzy, J., Rouille, S., and Kahn, D. (2004). FixJ-regulated genes evolved through promoter duplication in *Sinorhizobium meliloti*. *Microbiology* *150*, 2335-2345.
- Franceschini, A., Szklarczyk, D., Frankild, S., Kuhn, M., Simonovic, M., Roth, A., Lin, J., Minguez, P., Bork, P., von Mering, C., *et al.* (2013). STRING v9.1: protein-protein interaction networks, with increased coverage and integration. *Nucleic Acids Res* *41*, 29.
- Frueauf, J.B., Dolata, M., Leykam, J.F., Lloyd, E.A., Gonzales, M., VandenBosch, K., and Kieliszewski, M.J. (2000). Peptides isolated from cell walls of *Medicago truncatula* nodules and uninfected root. *Phytochemistry* *55*, 429-438.
- Geurts, R., and Bisseling, T. (2002). Rhizobium nod factor perception and signalling. *Plant Cell* *14*, S239-249.
- Geurts, R., Fedorova, E., and Bisseling, T. (2005). Nod factor signaling genes and their function in the early stages of Rhizobium infection. *Curr Opin Plant Biol* *8*, 346-352.
- Gorres, K.L., and Raines, R.T. (2010). Prolyl 4-hydroxylase. *Crit Rev Biochem Mol Biol* *45*, 106-124.
- Gryder, R.M., and Adams, E. (1970). Properties of the inducible hydroxyproline transport system of *Pseudomonas putida*. *J Bacteriol* *101*, 948-958.
- Hara, R., and Kino, K. (2009). Characterization of novel 2-oxoglutarate dependent dioxygenases converting L-proline to cis-4-hydroxy-l-proline. *Biochem Biophys Res Commun* *379*, 882-886.
- Honka, E., Fabry, S., Niermann, T., Palm, P., and Hensel, R. (1990). Properties and primary structure of the L-malate dehydrogenase from the extremely thermophilic archaeobacterium *Methanothermus fervidus*. *Eur J Biochem* *188*, 623-632.
- Jendrossek, D., Kratzin, H.D., and Steinbuchel, A. (1993). The *Alcaligenes eutrophus* *ldh* structural gene encodes a novel type of lactate dehydrogenase. *FEMS Microbiol Lett* *112*, 229-235.
- Karunakaran, R., Ramachandran, V.K., Seaman, J.C., East, A.K., Mouhsine, B., Mauchline, T.H., Prell, J., Skeffington, A., and Poole, P.S. (2009). Transcriptomic analysis of *Rhizobium leguminosarum* biovar *viciae* in symbiosis with host plants *Pisum sativum* and *Vicia cracca*. *J Bacteriol* *191*, 4002-4014.
- Khashimova, Z.S. (2003). Hydroxyproline-Containing Plant Proteins. *Chemistry of Natural Compounds* *39*,

229-236.

Knee, E.M., Gong, F.C., Gao, M., Teplitski, M., Jones, A.R., Foxworthy, A., Mort, A.J., and Bauer, W.D. (2001). Root mucilage from pea and its utilization by rhizosphere bacteria as a sole carbon source. *Mol Plant Microbe Interact* 14, 775-784.

Kumar, R., Zhao, S., Vetting, M.W., Wood, B.M., Sakai, A., Cho, K., Solbiati, J., Almo, S.C., Sweedler, J.V., Jacobson, M.P., *et al.* (2014). Prediction and Biochemical Demonstration of a Catabolic Pathway for the Osmoprotectant Proline Betaine. *mBio* 5.

Lam, H., Oh, D.C., Cava, F., Takacs, C.N., Clardy, J., de Pedro, M.A., and Waldor, M.K. (2009). D-amino acids govern stationary phase cell wall remodeling in bacteria. *Science* 325, 1552-1555.

Long, S.R. (2001). Genes and signals in the rhizobium-legume symbiosis. *Plant Physiol* 125, 69-72.

Maclean, A.M., White, C.E., Fowler, J.E., and Finan, T.M. (2009a). Identification of a hydroxyproline transport system in the legume endosymbiont *Sinorhizobium meliloti*. *Mol Plant Microbe Interact* 22, 1116-1127.

MacLean, A.M., White, C.E., Fowler, J.E., and Finan, T.M. (2009b). Identification of a Hydroxyproline Transport System in the Legume Endosymbiont *Sinorhizobium meliloti*. *Molecular Plant-Microbe Interactions* 22, 1116-1127.

Madern, D. (2002). Molecular evolution within the L-malate and L-lactate dehydrogenase super-family. *J Mol Evol* 54, 825-840.

Manoharan, T.H. (1980). Effect of glucose on induction of L-hydroxyproline dissimilatory pathway enzymes in *Pseudomonas aeruginosa* PAQ in presence of absence of ammonium sulphate. *Indian J Exp Biol* 18, 748-750.

Menzel, R., and Roth, J. (1981). Enzymatic properties of the purified putA protein from *Salmonella typhimurium*. *J Biol Chem* 256, 9762-9766.

Muirhead, R.P., and Hothersall, J.S. (1995). The effect of phenazine methosulphate on intermediary pathways of glucose metabolism in the lens at different glycaemic levels. *Exp Eye Res* 61, 619-627.

Muramatsu, H., Mihara, H., Goto, M., Miyahara, I., Hirotsu, K., Kurihara, T., and Esaki, N. (2005a). A new family of NAD(P)H-dependent oxidoreductases distinct from conventional Rossmann-fold proteins. *J Biosci Bioeng* 99, 541-547.

Muramatsu, H., Mihara, H., Kakutani, R., Yasuda, M., Ueda, M., Kurihara, T., and Esaki, N. (2005b). The putative malate/lactate dehydrogenase from *Pseudomonas putida* is an NADPH-dependent  $\Delta^1$ -piperideine-2-carboxylate/ $\Delta^1$ -pyrroline-2-carboxylate reductase involved in the catabolism of D-lysine and D-proline. *J Biol Chem* 280, 5329-5335.

Muramatsu, H., Mihara, H., Kakutani, R., Yasuda, M., Ueda, M., Kurihara, T., and Esaki, N. (2005c). The Putative Malate/Lactate Dehydrogenase from *Pseudomonas putida* Is an NADPH-dependent  $\Delta^1$ -Piperideine-2-carboxylate/ $\Delta^1$ -Pyrroline-2-carboxylate Reductase Involved in the Catabolism of d-Lysine and d-Proline. *Journal of Biological Chemistry* 280, 5329-5335.

Nishikawa, M., and Ogawa, K.i. (2004). Occurrence of d-histidine residues in antimicrobial poly(arginyl-histidine), conferring resistance to enzymatic hydrolysis. *FEMS Microbiology Letters* 239, 255-259.

Ostrovsky de Spicer, P., and Maloy, S. (1993). PutA protein, a membrane-associated flavin dehydrogenase, acts as a redox-dependent transcriptional regulator. *Proceedings of the National Academy of Sciences* 90, 4295-4298.

Pollegioni, L., Blodig, W., and Ghisla, S. (1997). On the mechanism of D-amino acid oxidase. Structure/linear free energy correlations and deuterium kinetic isotope effects using substituted phenylglycines. *J Biol Chem* 272, 4924-4934.

Radkov, A.D., and Moe, L.A. (2013). Amino acid racemization in *Pseudomonas putida* KT2440. *J Bacteriol* 195, 5016-5024.

Rathbun, E.A., Naldrett, M.J., and Brewin, N.J. (2002). Identification of a family of extensin-like glycoproteins in the lumen of rhizobium-induced infection threads in pea root nodules. *Mol Plant Microbe Interact* *15*, 350-359.

Riedel, T.J., Johnson, L.C., Knight, J., Hantgan, R.R., Holmes, R.P., and Lowther, W.T. (2011). Structural and biochemical studies of human 4-hydroxy-2-oxoglutarate aldolase: implications for hydroxyproline metabolism in primary hyperoxaluria. *PLoS ONE* *6*, 6.

Rigali, S., Derouaux, A., Giannotta, F., and Dusart, J. (2002). Subdivision of the helix-turn-helix GntR family of bacterial regulators in the FadR, HutC, MocR, and YtrA subfamilies. *J Biol Chem* *277*, 12507-12515.

Shibasaki, T., Mori, H., Chiba, S., and Ozaki, A. (1999). Microbial proline 4-hydroxylase screening and gene cloning. *Appl Environ Microbiol* *65*, 4028-4031.

Singh, R.M., and Adams, E. (1964). Alpha-Ketoglutaric Semialdehyde: A Metabolic Intermediate. *Science* *144*, 67-68.

Singh, R.M., and Adams, E. (1965). Enzymatic deamination of delta-1-pyrroline-4-hydroxy-2-carboxylate to 2,5-dioxovalerate (alpha-ketoglutaric semialdehyde). *J Biol Chem* *240*, 4344-4351.

Tamura, K., Stecher, G., Peterson, D., Filipiński, A., and Kumar, S. (2013). MEGA6: Molecular Evolutionary Genetics Analysis version 6.0. *Mol Biol Evol* *30*, 2725-2729.

Visser, W.F., Verhoeven-Duif, N.M., and de Koning, T.J. (2012a). Identification of a human trans-3-hydroxy-L-proline dehydratase, the first characterized member of a novel family of proline racemase-like enzymes. *J Biol Chem* *287*, 21654-21662.

Visser, W.F., Verhoeven-Duif, N.M., and de Koning, T.J. (2012b). Identification of a Human trans-3-Hydroxy-L-proline Dehydratase, the First Characterized Member of a Novel Family of Proline Racemase-like Enzymes. *Journal of Biological Chemistry* *287*, 21654-21662.

Watanabe, S., Morimoto, D., Fukumori, F., Shinomiya, H., Nishiwaki, H., Kawano-Kawada, M., Sasai, Y., Tozawa, Y., and Watanabe, Y. (2012). Identification and characterization of D-hydroxyproline dehydrogenase and Delta1-pyrroline-4-hydroxy-2-carboxylate deaminase involved in novel L-hydroxyproline metabolism of bacteria: metabolic convergent evolution. *J Biol Chem* *287*, 32674-32688.

Watanabe, S., Tanimoto, Y., Yamauchi, S., Tozawa, Y., Sawayama, S., and Watanabe, Y. (2014). Identification and characterization of trans-3-hydroxy-L-proline dehydratase and Delta(1)-pyrroline-2-carboxylate reductase involved in trans-3-hydroxy-L-proline metabolism of bacteria. *FEBS Open Bio* *4*, 240-250.

Watanabe, S., Yamada, M., Ohtsu, I., and Makino, K. (2007). alpha-ketoglutaric semialdehyde dehydrogenase isozymes involved in metabolic pathways of D-glucarate, D-galactarate, and hydroxy-L-proline. Molecular and metabolic convergent evolution. *J Biol Chem* *282*, 6685-6695.

White, C.E., Gavina, J.M., Morton, R., Britz-McKibbin, P., and Finan, T.M. (2012a). Control of hydroxyproline catabolism in *Sinorhizobium meliloti*. *Mol Microbiol* *85*, 1133-1147.

White, C.E., Gavina, J.M.A., Morton, R., Britz-McKibbin, P., and Finan, T.M. (2012b). Control of hydroxyproline catabolism in *Sinorhizobium meliloti*. *Molecular Microbiology* *85*, 1133-1147.

Wu, G., Bazer, F.W., Burghardt, R.C., Johnson, G.A., Kim, S.W., Knabe, D.A., Li, P., Li, X., McKnight, J.R., Satterfield, M.C., *et al.* (2011). Proline and hydroxyproline metabolism: implications for animal and human nutrition. *Amino Acids* *40*, 1053-1063.

Yoneya, T., and Adams, E. (1961). Hydroxyproline metabolism. V. Inducible allohydroxy-D-proline oxidase of *Pseudomonas*. *J Biol Chem* *236*, 3272-3279.

Zhao, S., Kumar, R., Sakai, A., Vetting, M.W., Wood, B.M., Brown, S., Bonanno, J.B., Hillerich, B.S., Seidel, R.D., Babbitt, P.C., *et al.* (2013). Discovery of new enzymes and metabolic pathways by using structure and genome context. *Nature* *502*, 698-702.